

The Therapeutic Potential of Ginger and/or Glucosamine Sulfate on Adjuvant- Induced Rheumatoid Arthritis in Adult Rats; an Anatomical, Histological and Biochemical Study

Rehab A. Abd-El-Moneim¹, Marwa Mahmoud Mady², Mona Hassan Fathelbab³ and Heba F. Ibrahim¹

¹Department of Histology and Cell Biology, ²Department of Human Anatomy and Embryology, ³Department of Medical Biochemistry, Faculty of Medicine, Alexandria University, Egypt

ABSTRACT

Introduction: Rheumatoid arthritis (RA) is a common health problem with a serious impact on quality of life. Hence, variable therapeutic regimens have been tested to ameliorate the symptoms and hinder the disease progression.

Aim of the Work: To assess the therapeutic effect of ginger (GR) or glucosamine sulfate (GAS) separately versus their combined administration in a rat model of induced-RA.

Materials and Methods: Sixty adult female albino rats were allocated into five groups; 20 rats were the control group I. RA was induced by a single intra-articular injection of 100 µL of Complete Freund's Adjuvant (CFA) in the knee joints of the remaining forty rats, then distributed after 7 days into: RA group II, GR group III (received 400 mg GR/kg/day), GAS group IV (received 250 mg GAS/kg/day), and combined treatment group V. Treatment groups were euthanized after 28 days. Assessment of serum levels of tumor necrosis factor-alpha (TNF-α) and interleukin-6 (IL-6) was done. Right knee joints were dissected for gross macroscopic and scanning electron microscope (SEM) examinations. Left knee joints were processed for a histological examination by hematoxylin and eosin (H & E) and Masson's trichrome stains.

Results: In group V, serum levels of TNF-α and IL-6 restored nearly their control values. Gross and SEM examinations revealed mostly regular articular cartilage surfaces. Histologically, mostly smooth cartilage surfaces were observed with preserved joint space and distinct cartilage zones, in comparison to GR and GAS treated groups that exhibited limited surface irregularities and invasion of the joint space by pannus tissue, in some sections. Trichrome stained sections demonstrated a significant decline in percentage area of collagen within the pannus in group V as compared to RA group.

Conclusion: The combined treatment enhanced the therapeutic effect of GR and GAS, thus resulted in the most prominent improvement in all assessed parameters.

Received: 30 July 2022, **Accepted:** 23 August 2022

Key Words: Ginger, glucosamine sulfate, pannus, rheumatoid arthritis.

Corresponding Author: Heba F. Ibrahim, PhD, Department of Histology and Cell Biology, Faculty of Medicine, Alexandria University, Egypt, **Tel.:** +20 10 2941 6546, **E-mail:** hebafathyibrahim@gmail.com - heba.fathy15@alexmed.edu.eg

ISSN: 1110-0559, Vol. 46, No. 4

INTRODUCTION

Arthritis is considered as a common health problem that affects millions of people worldwide, where osteoarthritis (OA) and rheumatoid arthritis (RA) represent the two major types of arthritis that are associated with severe joint pain, restricted mobility and a reduced quality of life^[1].

Rheumatoid arthritis (RA) is an autoimmune systemic condition that involves immune dysregulation and inflammation, thereby causing articular cartilage deformity. Such an effect involves multiple joints, leading to evident disabilities. Female gender, genetics, and smoking are among the most important risk factors for developing RA^[2]. Therefore, female albino rats were chosen to be the experimental model for induction of RA in the current study.

The presence or absence of antibodies helps to classify RA into a seropositive or seronegative disease. Seropositive

patients have more severe inflammation and joint damage over the course of the disease, the issue that eventually ends up in a permanent deformity^[3,4]. Overall, RA patients confront a high rate of disability, with approximately 60% of them are unable to work after just 10 years of the disease onset^[4]. Symptoms of RA include tender, warm and swollen joints as well as morning stiffness and inactivity^[5].

The pathogenesis of RA is actually multifactorial, where it is documented that several inflammatory cytokines are related to eliciting the inflammatory reaction in RA, such as, interleukins-1, 6 (IL-1, 6) and tumor necrosis factor- alpha (TNF-α). Other factors that play a role in the disease pathogenesis include nitric oxide (NO), matrix metalloproteinases (MMPs), and prostaglandin E-2 (PGE-2). Collectively, all these factors induce several catabolic events in the different joint components, leading to synovitis^[6].

Despite of the modern advances in the medical knowledge, it is difficult to provide an effective and safe treatment for RA. The American College of Rheumatology/Arthritis Foundation recommends usage of some possible treatment options that include; oral and topical non steroidal anti-inflammatory drugs (NSAIDs), oral analgesics, serotonin and norepinephrine reuptake inhibitors and intra-articular corticosteroids. However, these pharmacological drugs impart hazardous health effects such as gastrointestinal, cardiovascular and nephro-toxicities^[1,7-9]. Therefore, it has been a challenging issue to search for more effective and safer therapeutic regimens.

In this regard, natural supplements such as, glucosamine (GA) and ginger (GR) have been implemented as possible effective therapeutic agents that target the disease pathogenesis; in a trial to hinder its progression. Glucosamine is an amino monosaccharide that is found naturally in the connective tissue and cartilage. Moreover, large amounts of it can be produced for the commercial purposes from wheat and corn^[10]. It was reported that glucosamine sulfate (GAS) could improve the joint function and reduce pain in patients suffering from osteoarthritis^[11,12], thus it could be also introduced as a possible therapeutic alternative for RA.

On the other hand, herbal medicine is emerging as a safer treatment strategy for RA. Zingiberofficinale- commonly known as ginger (GR) is a flowering plant that is used as a dried herbal or a food cooking flavor, especially in Asia. It has been used to treat dyspepsia, nausea, vomiting, diarrhea, high blood pressure, muscle aches, asthma and arthritis, owing to its strong anti-inflammatory, antibacterial and antioxidant properties. These effects of GR have been extensively studied whether in patients or animal models^[13,14].

In such a context, the current study aimed to investigate the therapeutic effects of GR and GAS in an experimental model of RA. Moreover, it was within the scope of the study to compare between their combined therapeutic efficiency versus the effect of each of them individually.

MATERIAL AND METHODS

Animals and experimental design

Sixty adult female Sprague-Dawley albino rats, weighing 200-250 g, at 8-12 weeks of age, were enrolled in the present study. The rats were raised at the Animal House of Physiology Department, Faculty of Medicine, Alexandria University. Rats were handled in a strict accordance with the institutional ethical committee guidelines for care and use of laboratory animals. The approval of the ethics committee was recorded by IRB NO. 000112098- FWA NO. 00018699. Each rat had a free access to water and standard rodent soft chow.

After acclimatization for 2 weeks, the rats were randomly divided as follows

Group I (control group): 20 rats which were further subdivided into;

- Group IA: 10 rats were not subjected to any treatment and served as negative control group.
- Group IB: 10 rats were subjected to a single intra-articular injection of 100 µL of paraffin mineral oil (vehicle of the bacteria in the Complete Freund's adjuvant "CFA") in each knee joint and were left for 35 days (the entire duration of the experiment).

The other forty rats were subjected to a single intra-articular injection of 100 µL of CFA, in each knee joint, to induce the RA model^[15]. Seven days after the injection, rats were randomly allocated into the following groups:

Group II (RA group): 10 rats were euthanized seven days after the injection to ensure the development of the RA.

Group III (GR group): 10 rats received 400 mg/kg/day of GR dissolved in 1 ml of distilled water via orogastric tube, for 28 days^[16].

Group IV (GAS group): 10 rats received 250 mg/kg/day of GAS dissolved in 0.7 ml of distilled water via orogastric tube, for 28 days^[17].

Group V (the combined group): 10 rats received 400 mg/kg/day of GR in addition to 250 mg/kg/day of GAS, simultaneously, for 28 days in the same previously mentioned mode of administration.

Induction of rheumatoid arthritis (RA)

Under sterile conditions, adjuvant induced arthritis (AIA) model was induced by a single intra-articular injection of freshly prepared 100 µL of CFA (heat killed mycobacterium butyricum in paraffin mineral oil "1mg/ml", Sigma, St. Louis, MO 63103, USA; cat #12512) into each knee of each rat^[15].

Therapeutic agents

GR (500 mg/capsule) and GAS (500 mg/capsule) were commercially purchased as supplements from the pharmacy. The capsules' content was dissolved in distilled water for their oral administration.

Biochemical pro-inflammatory cytokines assessment

Blood samples were collected from the retro orbital plexus of veins from all rats, into plain tubes before animals' euthanization. Blood samples were allowed to clot for 2 hours at room temperature before centrifugation for 20 minutes at 1000 xg. Serum samples were separated and kept frozen at -80oC until use.

The serum levels of interleukin-6 (IL-6) were measured using Quantikine® rat IL-6 immunoassay (Catalog Number R6000B, R&D Systems, Minneapolis, MN, USA) and tumor necrosis factor- alpha (TNF-α)(Catalog Number RTA00, R&D Systems, Minneapolis, MN, USA) were assessed by using ELISA kits according to the manufacturer's instructions. The colour intensity was in proportion to the amount of the measured substance, and the measurement was at 450 nm. Samples were analysed in duplicate and results were expressed in pg/mL^[18,19].

Anatomical and histological studies

Gross macroscopic assessment

Rats of different groups were euthanized at the end of the decided duration for each group. Dissection of both knee joints from each rat was performed through stripping off the covering skin, followed by removal of the underlying soft tissues carefully. In a following step, the knee joints were completely separated by being cut at mid-femur and mid-tibia regions. The right knee joints of rats from all groups were immediately fixed in 4F1G (4% formaldehyde and 1% glutaraldehyde) solution. Finally, the articular surfaces of both femur and tibia were disclosed through meticulous removal of tendons and ligaments^[20].

Gross macroscopic examination of the articular cartilage surfaces of the femoral condyles and the tibial plateaus was done. They were then photographed using Olympus SZ dissecting stereomicroscope (Olympus-Japan), at the Experimental Embryology Lab, Anatomy and Embryology department, Faculty of Medicine, Alexandria University^[21,22]. The gross appearance of the articular surfaces was blindly scored by the system, set by Yoshimi *et al.*,^[23] on a scale ranging from 0 to 5. The following parameters were included in this scoring system; 0: normal and smooth articular surface, 1: surface irregularities, 2: surface fibrillations (superficial cartilage erosions), 3: partial cartilage erosion (exposing the subchondral bone), 4: ulceration (full thickness erosion of the cartilage), 5: complete cartilage loss.

Scanning electron microscope (SEM) assessment

The right knee joints that were subjected to gross macroscopic examination, were re-immersed in 4F1G solution, then processed for examination by a Joel scanning electron microscope (JSM-IT200, In touch scope series), at the electron microscope unit, faculty of Science, Alexandria university^[24]. The SEM examination targeted assessment of the articular cartilage surface topography for any abnormalities.

Light microscopic assessment

The intact left knee joints were preserved in neutral buffered formalin (10% formaldehyde). After 48 hours, samples were immersed in 20% ethylene diamine tetra acetic acid (EDTA) and left for two weeks, for decalcification. Then, the samples were processed for preparation of paraffin blocks and obtainment of sagittal sections with 5-6 μm thickness. The sections were then stained with hematoxylin and eosin (H&E) to evaluate the structural degenerative and inflammatory changes of the cartilage and joint cavity. Other sections were stained by Masson's trichrome stain for assessment of collagen deposition within the synovium^[25,26]. The sections were examined and photographed by using a light microscope (Olympus BX41, Tokyo, Japan), equipped with digital camera (Olympus DP20, Tokyo, Japan), at the Centre of Excellence of Research in Regenerative Medicine and its Applications (CERRMA), Faculty of Medicine, Alexandria University.

Morphometric analysis

The Masson's trichrome stained sections were subjected to a morphometric analysis through measurement of the percentage of collagen stained areas that exhibited a bluish green colour, in photographed sections at magnification of 100, in five randomly selected sections from each group. NIH Fiji© software program (version 1.51k, Wayne Rasband, National Institutes of Health, Maryland, USA), was used^[27].

Biostatistical analysis

Data from biochemical and morphometric assessments were fed to the computer and analyzed using IBM SPSS software package version 20.0. (Armonk, NY: IBM Corp). The Shapiro-Wilk test was used to verify the normality of distribution. Quantitative data were described using range (minimum and maximum), mean and standard deviation. Significance of the obtained results was judged at the 5% level. The used tests were one way ANOVA test for normally distributed quantitative variables, to compare between more than two groups, and Post Hoc test (Tukey) for pairwise comparisons^[28].

RESULTS

Biochemical results

Statistically, all the results of group IA were not significantly different from group IB. Therefore, we considered them collectively as the control group. The mean serum level of IL-6 in the control group was about 64.80 pg/ml, while its level in the RA group was significantly increased to reach 161.2 ± 12.11 pg/ml. Such a result supports the occurrence of an inflammatory reaction. Meanwhile, the different treatment groups (III, IV & V), demonstrated a significant decline in the IL-6 serum levels, in comparison to RA group with a *P value* ≤ 0.001 . However, the combined treatment in group V, restored nearly the control IL-6 serum level, as it was insignificant as compared to the control group with a *P value* of 0.035 (Table 1, Figure 1).

The mean serum level of TNF- α in the control group was 54.80pg/ml, demonstrating a significant rise in RA group (group II) to reach 117.0 ± 10.68 pg/ml. A significant decrease of TNF- α serum levels was achieved by all the treatment groups as compared to the RA group with a *P value* ≤ 0.001 . However, group V (combined treatment group), demonstrated TNF- α serum level that was insignificant from the control group with a *P value* = 0.618. Meanwhile, groups III (GR) and IV (GAS), were still revealing significantly increased TNF- α serum levels in comparison to the control group (Table 2, Figure 2).

Gross macroscopic results

The articular surfaces of the cartilage of the right femur and tibia were examined and grossly scored for assessing the degree of degeneration. Knee joints from rats of the control group showed normal appearance of the articular cartilage of both femur and tibia. They exhibited Yoshimi

gross anatomical score of zero. The surfaces of the articular cartilage were smooth, regular and shiny showing no evidence of degeneration (Figure 3, Table 3).

In group II (RA model), the articular cartilage illustrated surface ulcerations. The mean macroscopic score was 3.80 which is significantly higher than the mean of the control group (Figure 3, Table 3).

The articular cartilages of GR group revealed gross changes ranging from surface irregularities to fibrillations. The mean macroscopic score was 2.30 which is significantly high in comparison with the control group. Group IV (GAS group) exhibited areas of fibrillations together with ulcerations. The mean of its macroscopic scores was 2.0, which is significantly high in comparison with the control group. However, knee joints of the combined group showed apparent restoration of the normal appearance of articular cartilage with just focal areas of irregularities in the femoral condyles. The mean macroscopic score of this group was 0.8, with no significant difference from the mean of the control group (Figure 4, Table 3).

Collectively, the mean of the combined group was significantly less than the means of groups III and IV. Each of group III and group IV demonstrated relative improvement in comparison to the RA group, where their mean scores were significantly lower (Table 3).

Scanning electron microscope (SEM) results

Control group I: The right femoral condyles exhibited smooth articular cartilage surfaces (Figure 5).

Group II (RA group): Articular cartilage surface of the right femoral condyles of the RA model group II revealed some areas with multiple surface discontinuities in the form cracks and fissures. Some other areas exhibited irregular rough surface with evident raised parts and depressions (Figure 6).

Group III (GR treated): The right femoral condyles exhibited mostly smooth articular surface with focal cracks and fissures. Mild elevations and depressions were observed in focal areas, meanwhile most of the articular surface depicted smooth appearance (Figure 7).

Group IV (GAS treated): Partial improvement was noticed, where some cracks and fissures were still observed, together with less evident roughness. Some areas revealed prominent elevations and depressions (Figure 8).

Group V (combined treatment): Evident restoration of apparently smooth surface of the femoral condyles was observed. However, focal areas of roughness were still noticed (Figure 9).

Light microscopic results

H & E results

Control group I: The articular cartilage depicted regular surfaces with scattered chondrocytes in their lacunae within a homogenous basophilic matrix. In addition, cell nests

were observed. Different zones of the articular cartilage; superficial, middle, deep and calcified cartilage zones were distinguished, together with an evident tidemark line between the deep zone and underlying calcified zone. The joint space appeared preserved (Figure 10).

Group II (RA model): The articular cartilage exhibited variable degenerative changes. In some sections, it appeared thinned out with areas of superficial discontinuity. Evident invasion of the joint space with proliferated synovial tissue (pannus tissue) and inflammatory cellular infiltration was noticed, with partial interruption of the cartilage surface and extension of the pannus tissue into the cartilage matrix in some parts. Erosion of the subchondral bone was observed in some other sections. In addition, some chondrocytes exhibited vacuolated cytoplasm and dark eccentric nuclei. The different zones of the articular cartilage were not well distinguished, with mostly indistinct tidemark line. Vascular congestion and evident cellular infiltration were noticed within the pannus, together with a marked increase of the fibroblasts. Examination of the tissue sections at high power revealed that the cellular infiltration was composed of neutrophils, lymphocytes, eosinophils and plasma cells (Figures 11,12).

Group III (GR treated group): Apparent amelioration was observed, where the joint space appeared mostly preserved in some sections with limited pannus infiltration. Meanwhile, some other sections depicted evident invasion of the joint space with pannus tissue, together with erosion of the articular cartilage. In such sections, pannus tissue showed vascular congestion and marked cellular infiltration that was mostly composed of fibroblasts, few lymphocytes and few neutrophils. Focal areas of irregularities of the articular cartilage surfaces were also observed. Obvious zonation and tidemarks were seen in most of the sections, with only focal areas of indistinct zonation and tidemarks. Few areas of hypocellularity were observed, otherwise cartilage matrix exhibited cell nests and homogenous matrix (Figure 13).

Group IV (GAS treated group): Partial improvement was noticed, where the articular cartilage surfaces appeared mostly regular. Distinct zonation was observed within the cartilage, together with evident tidemarks. Moreover, chondrocytes within cell nests were frequently observed within homogenous matrix. Limited infiltration of the joint space with pannus tissue was seen in some sections. However, cellular infiltration was still encountered within the pannus, where most of the cells were fibroblasts (Figure 14).

Group V (combined treatment group): The most evident amelioration of the inflammatory and degenerative changes was observed in this group. Articular cartilage nearly restored the normal histological features, where limited pannus infiltration into the joint space was seen. In addition, articular cartilage surface depicted regular surface, except for some focal irregularities. Different zones of the cartilage were well distinguished, together with evident tidemark (Figure 15).

Masson's trichrome results and its morphometric analysis

Light microscopic examination of the trichrome stained sections revealed normal pattern of collagen distribution within synovium of the control group that exhibited limited green stained areas. Meanwhile, apparently increased collagen green stained areas were observed in RA group II. However, different treatment groups III, IV and V displayed apparently diminished collagen green stained areas (Figures 16,17).

Statistical analysis of the morphometric results of the collagen percentage area demonstrated a significant increase in all the studied groups in comparison with the control group ($P \leq 0.05$). However, it was decreased in the GR and GAS groups in comparison with the RA group, but not significantly. When the GR and GAS were administrated together in the combination group, the collagen percentage area decreased significantly in comparison with the RA group, denoting their synergetic effect in decreasing the collagen deposition ($P \leq 0.05$) (Figure 18, Table 4).

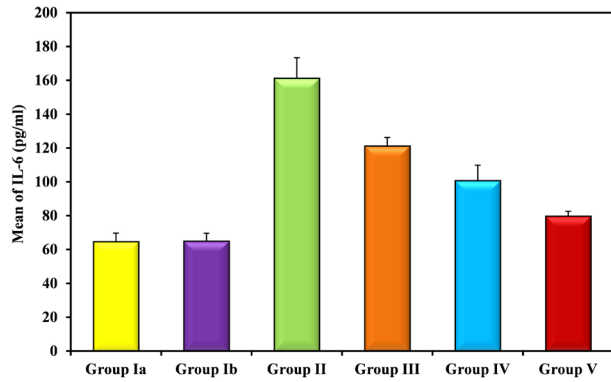


Fig. 1: Bar chart representing a comparison between the different studied groups according to serum IL-6 (pg/ml).

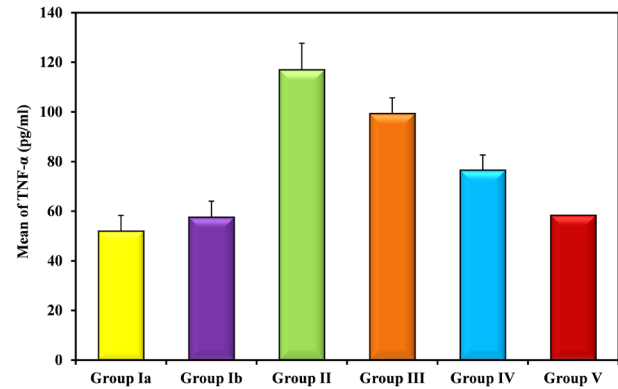


Fig. 2: Bar chart representing a comparison between the different studied groups according to serum TNF-α (pg/ml).

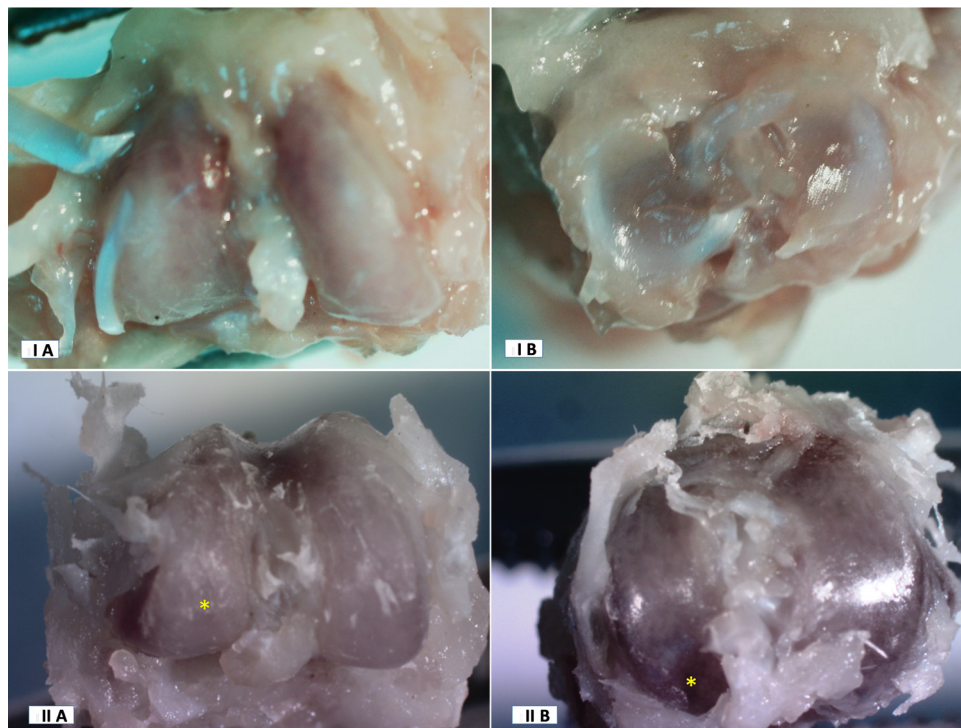


Fig. 3: Representative macroscopic images of the articular surfaces of femoral (A) and tibial (B) condyles. IA & IB (control group); show regular normal intact smooth cartilage of both medial and lateral condyles. IIA & IIB (RA group II); show areas of ulcerations and cartilage loss (asterisks). Microscopic (Mic) magnification (Mag) IA, IB, IIA, IIB x 4.

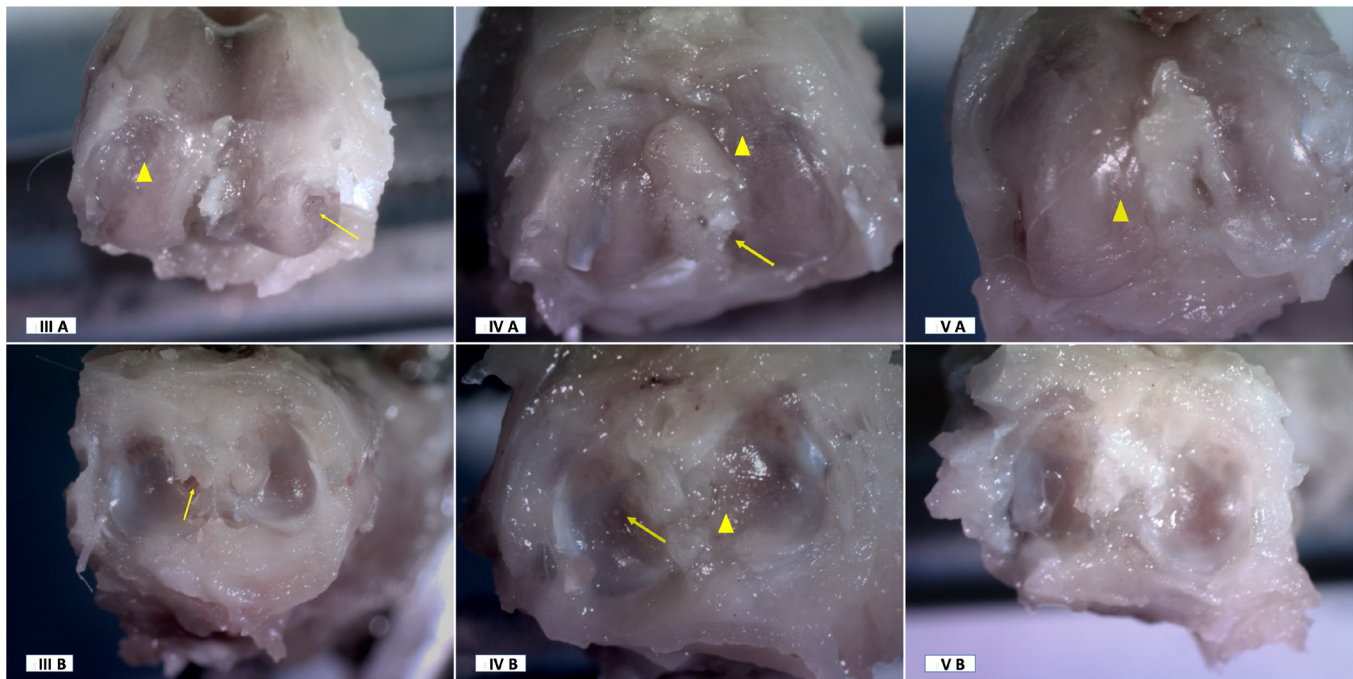


Fig. 4: Representative macroscopic images of the articular surfaces of femoral (A) and tibial (B) condyles of different treatment groups. IIIA & IIIB (GR group III); reveal surface irregularities (arrowhead) and fibrillations (arrows). IVA & IVB (GAS group IV); reveal surface irregularities (arrowheads) and fibrillations (arrows). VA & VB (combined group V); The articular surfaces of both bones show restoration of normal appearance of articular cartilage with just focal areas of irregularities in the femoral condyles (arrowhead). Mic. Mag. IIIA-VB x 4.

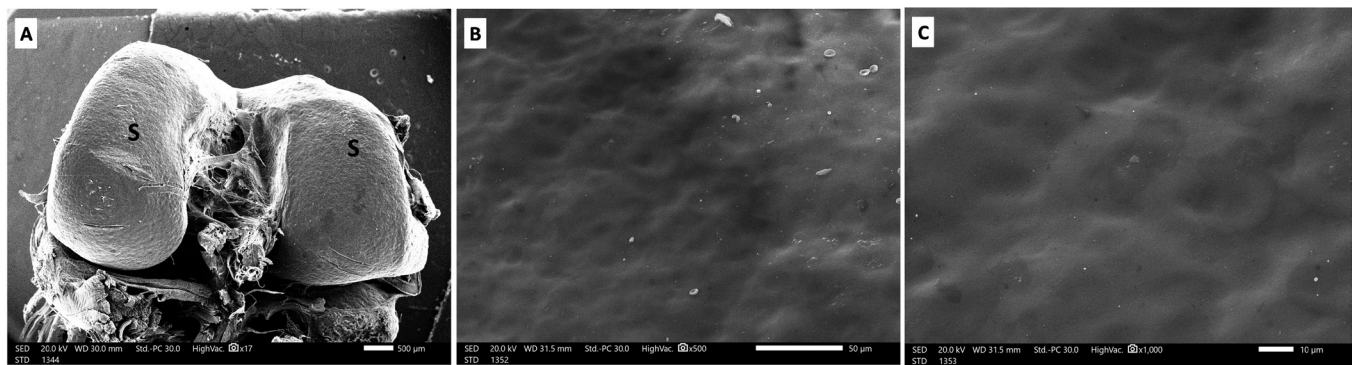


Fig. 5: (A-C): Representative SEM micrographs of the right femoral condyles' articular cartilage surfaces of the control group. A; Smooth cartilage surface (S) is exhibited. B & C; Higher magnifications reveal evident surface smoothness. Mic. Mag. A x 17, B x 500, C x 1000.

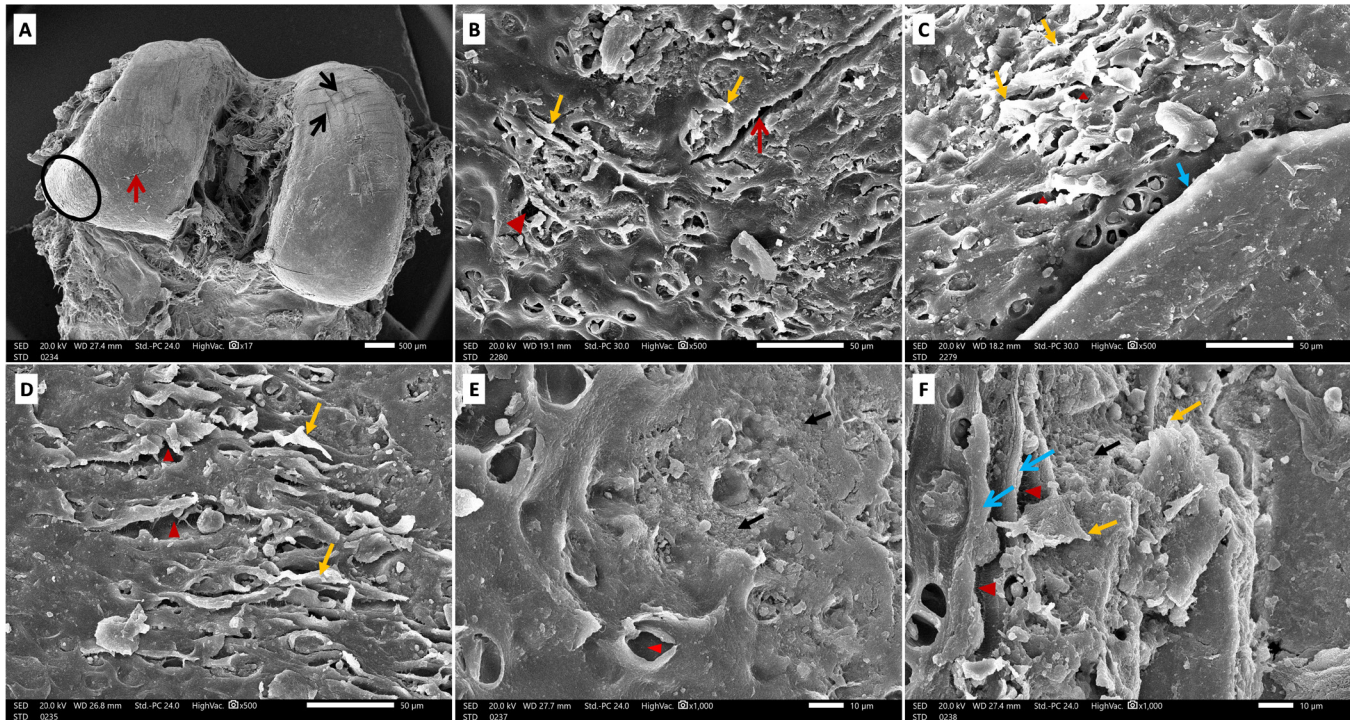


Fig. 6: (A-F): Representative SEM micrographs of the right femoral condyles' articular cartilage surface of RA group II. A; The articular surface exhibits multiple cracks (black arrows) and fissure (red arrow). Surface roughness (oval outlined) is observed. B; A higher magnification of the fissure (red arrow) in micrograph A is illustrated, together with multiple raised areas (yellow arrows) and pits (red arrowhead). C; A higher magnification of the oval outlined area in A, exhibits surface roughness to be formed of several raised ridge-like areas (blue arrow) or spike like parts (yellow arrows) and depressed parts (red arrowheads). D; Surface irregularities are displayed in the form of spike like elevations (yellow arrows) and downwards invaginations (red arrowheads). E & F; Evident surface roughness is observed (black arrows) together with depressed parts (red arrowheads) F; Ridge like areas (blue arrows) alternating with longitudinal depressions (red arrowheads) are noticed. Spike like elevations (yellow arrows) are also seen. Mic Mag A x 17, B, C & D x 500, E & F x 1000.

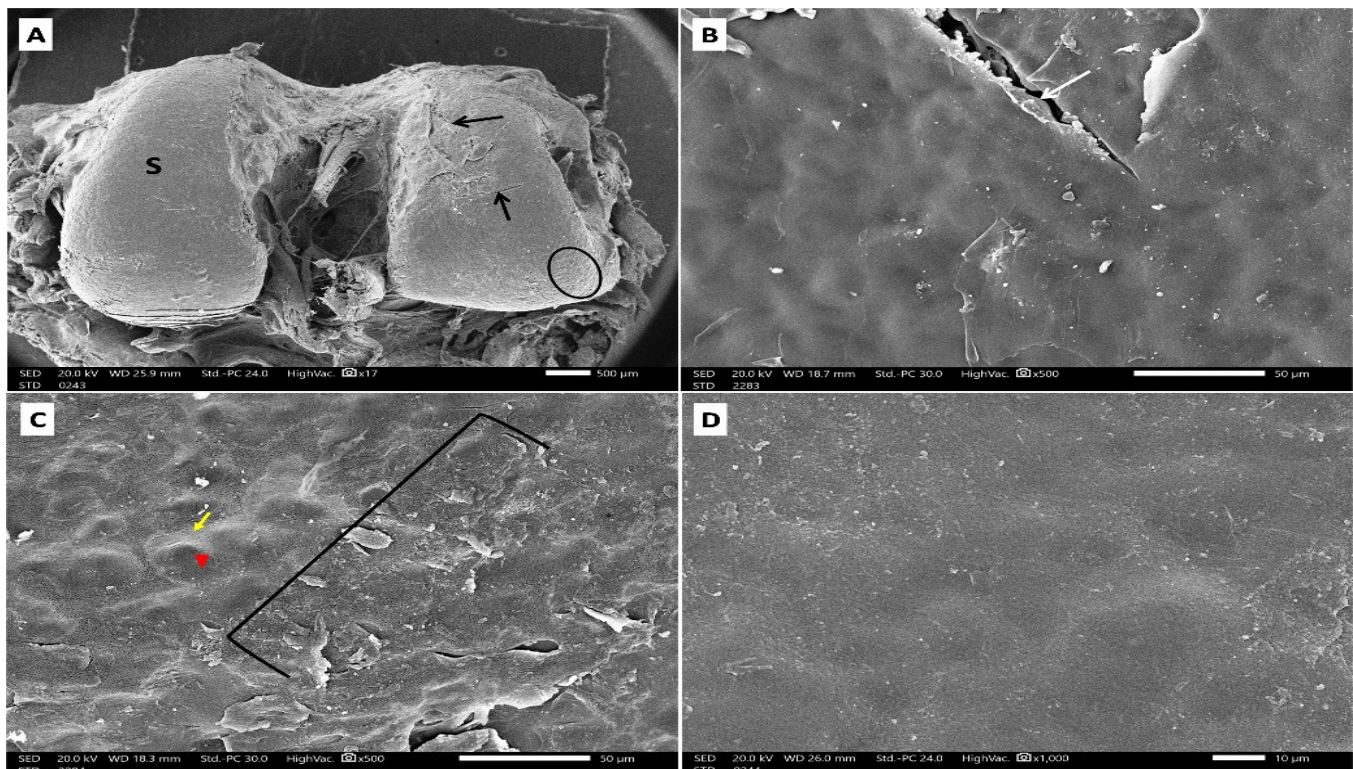


Fig. 7: (A-D). Representative SEM micrographs of right femoral condyles' articular cartilage surfaces of GR treated group III. A; Surface roughness (oval outlined) and some fissures (black arrows) are observed. Other areas exhibit smooth surface (S). B; A higher magnification micrograph of A reveals one of the fissures as an evident longitudinal surface discontinuity (white arrow). C; A higher magnification of the oval outlined area in A, reveals evident surface irregularities (bracket). Another area shows mild surface irregularities in the form of limited raised parts (yellow arrow) or invaginated part (red arrowhead). D; A higher magnification of the smooth surface (S) in micrograph A is confirmed. Mic Mag A x 17, B & C x 500, D x 1000

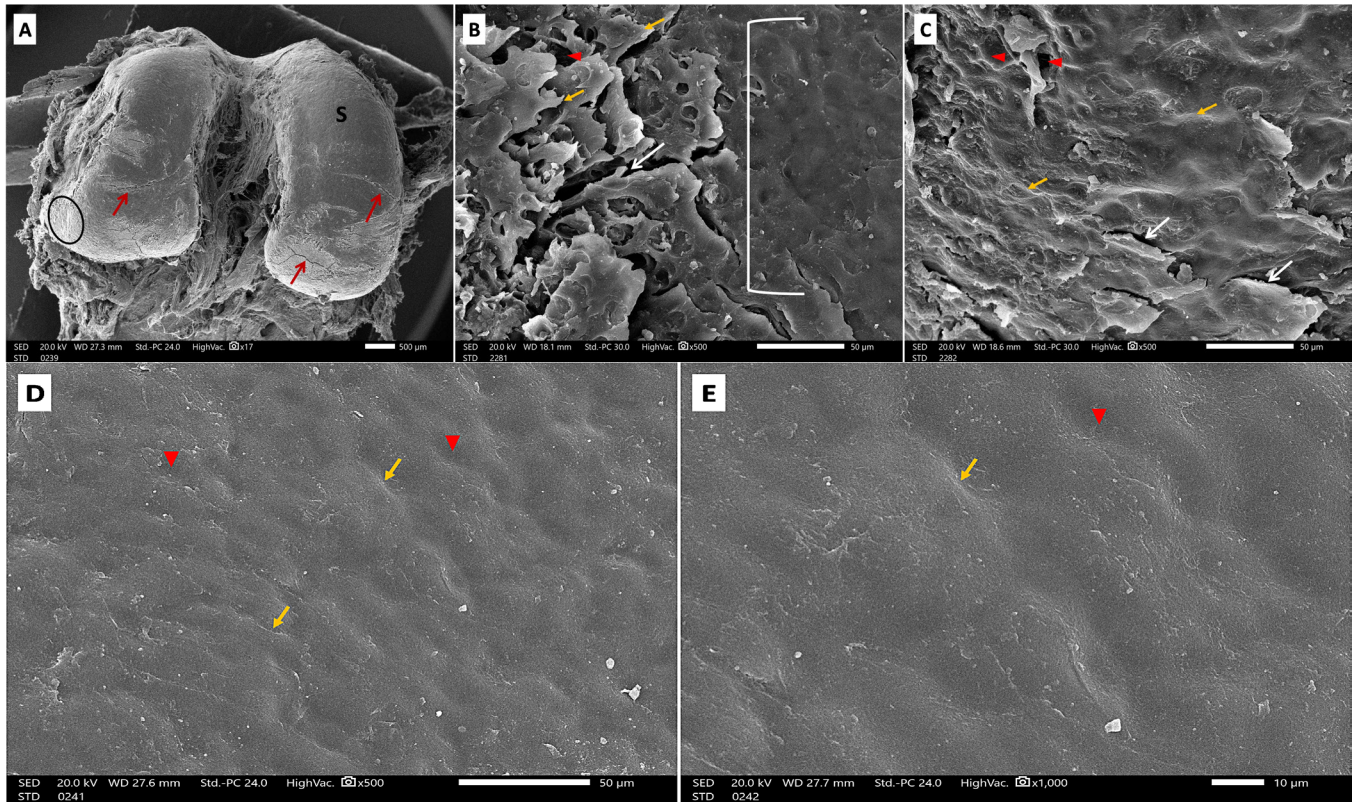


Fig. 8: (A-E). Representative SEM micrographs of right femoral condyles' articular cartilage surfaces of GAS treated group IV. A; Some areas of the surface depict roughness (oval outlined) or fissures (red arrows). Some other areas appear relatively smooth (S). B; At a higher magnification, the surface roughness is displayed as spike like elevations (yellow arrows) and depressions (red arrowheads). Longitudinal groove (white arrow) is noticed. Another area exhibits nearly smooth surface (bracket). C; Another area reveals milder raised parts (yellow arrows) and less eminent invaginations (red arrowheads). Longitudinal grooves (white arrows) are observed. D & E; Some parts display nearly smooth surface with mild irregularities in the form of limited eminence (yellow arrows) or shallow invaginations (red arrowheads). Mic Mag A x 17, B, C & D x 500, E x 1000.

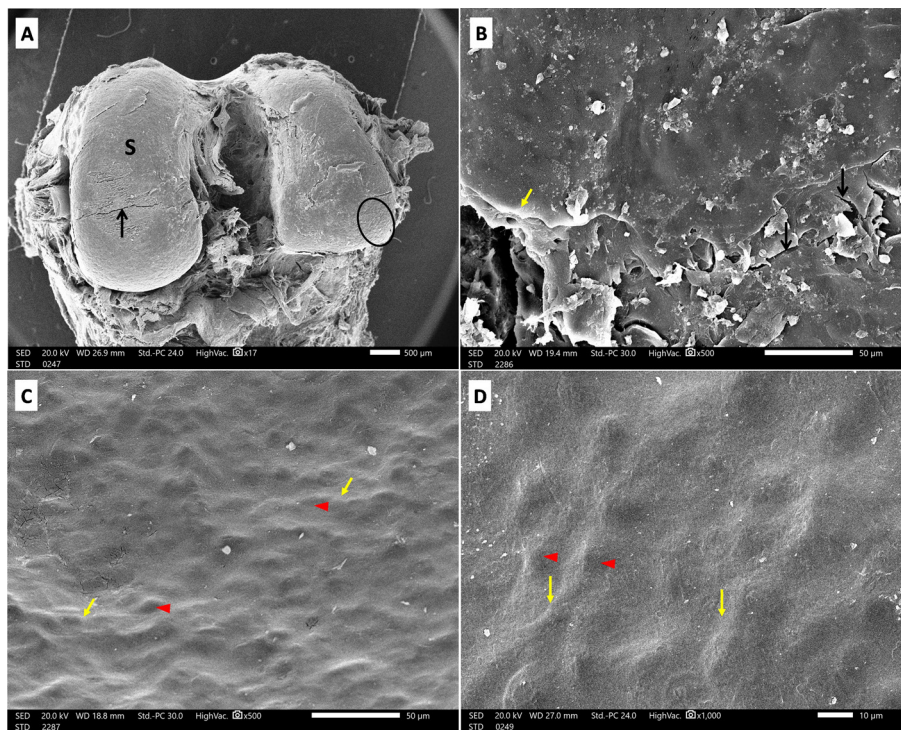


Fig. 9: (A-D): Representative SEM micrograph of the right femoral condyles' articular cartilage surface in the combined treatment group V. A; The articular surface exhibits mostly regular appearance (S). Focal fissure (black arrow) is observed. Limited surface roughness is illustrated in the oval outlined area. B; A higher magnification of the fissure area in (A) displays limited surface discontinuities (black arrows) and mildly raised area (yellow arrow). C & D; Smoothness of the surface is confirmed at higher magnifications. Limited elevations (yellow arrows) or depressed areas (red arrowheads) are seen. Mic Mag A x 17, B & C x 500, D x 1000

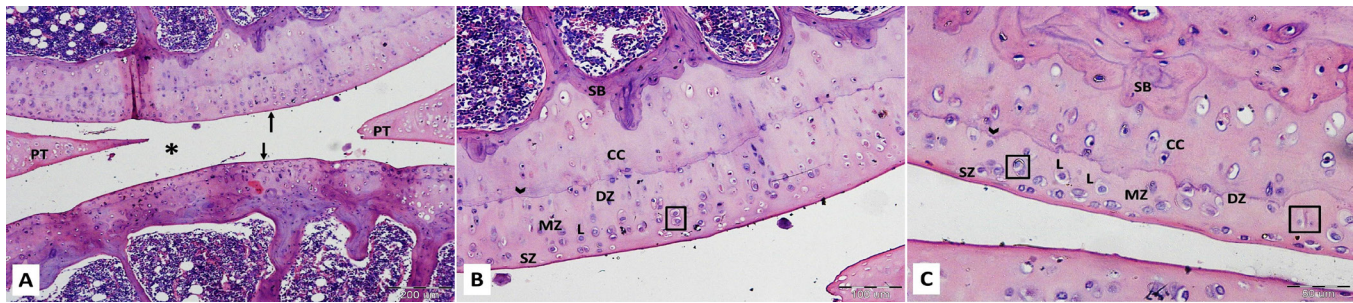


Fig. 10: (A-C): Representative LM pictures of the H & E stained sections of the control group I. A; Joint space appears empty (asterisk) and the articular cartilage exhibits normal thickness and smooth regular surface (arrows). The patella is apparent (PT). B & C; The higher magnifications show the different zones of the articular cartilage; superficial zone (SZ), mid zone (MD), deep zone (DZ) and calcified cartilage (CC). The underlying subchondral bone (SB) is also evident. The tidemark is clearly defined (arrowhead). The chondrocytes appear either scattered within their lacunae (L) or forming cell nests (rectangles). Mic Mag A x 100, B x 200, C x 400.

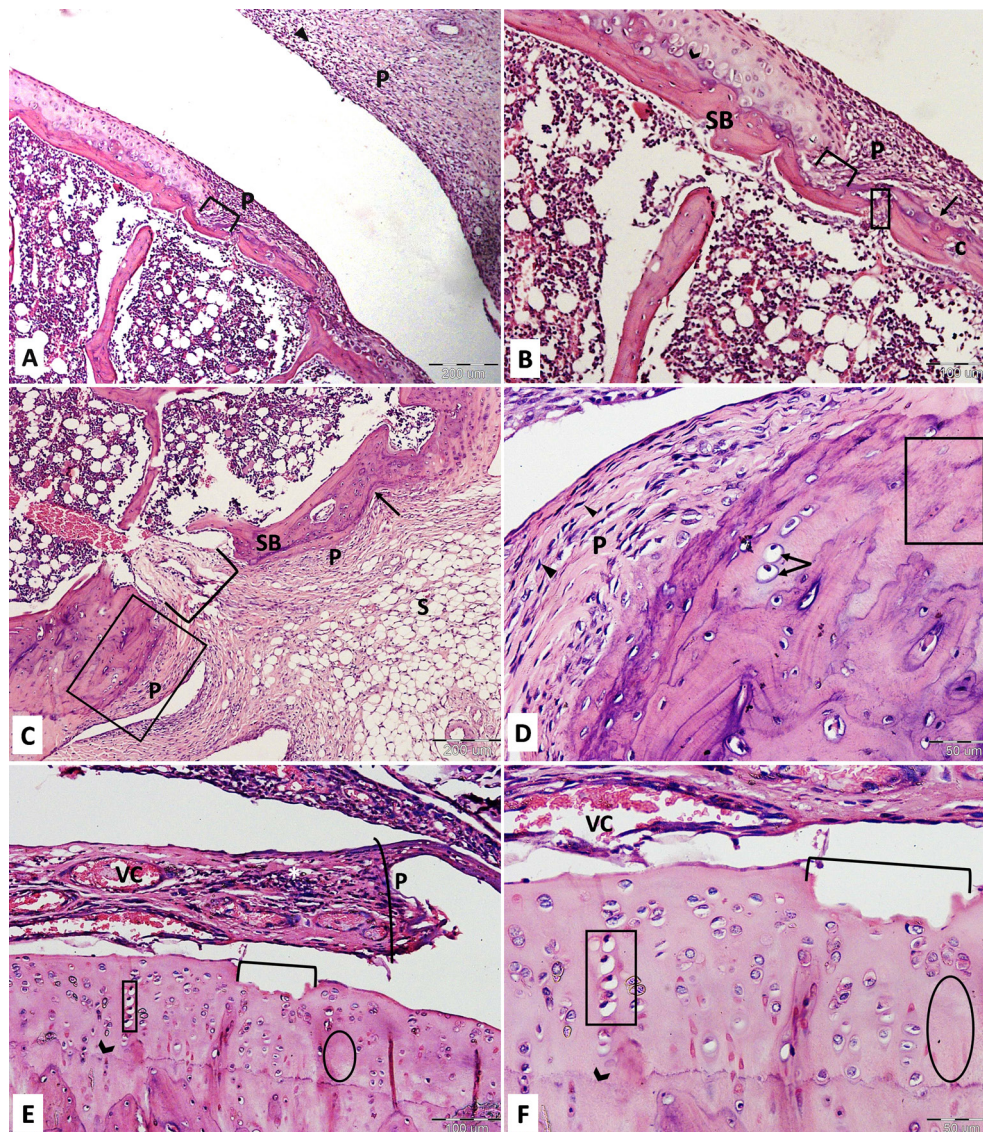


Fig. 11: (A-F): Representative LM pictures of the H & E stained sections of the RA model group II. A & B; Joint space appears invaded by pannus tissue (P) together with mononuclear cellular infiltration (triangle). Interruption of the cartilage continuity (bracket) is observed. B; A higher magnification of picture A, shows areas of decreased cartilage thickness (arrow). Subchondral bone (SB) shows discontinuity (rectangle) & an erosion cavity (c). Indistinct tidemark (arrowhead) & zones of the articular cartilage are noticed. Mic Mag A x 100, B x 200. C; Encroachment and depression of the cartilage surface (arrow) by the pannus tissue (P). Discontinuity of cartilage and SB (bracket) is noticed. D; A higher magnification of outlined area by the rectangle in picture (C) reveals spindle shaped cells with flat nuclei (arrowheads) that are suggestive of fibroblasts within the pannus tissue (synoviocytes). Vacuolated chondrocytes with eccentric darkly stained nuclei (arrows) are seen. Cartilage matrix depicts some areas of hypocoellularity (rectangle). Mic Mag C x 100, D x 400. E & F; Invasion of the joint space with pannus tissue (P) that exhibits vascular congestion (VC) & mononuclear cellular infiltration (asterisk). Notice discontinuity of cartilage surface with apparent partial loss of cartilage (bracket). Some areas of the matrix reveal hypocoellularity (oval shape). Some chondrocytes appear with vacuolated cytoplasm & eccentric dark nuclei (rectangle). Indistinct tidemark (arrowhead) is noticed. Mic Mag E x 200, F x 400.

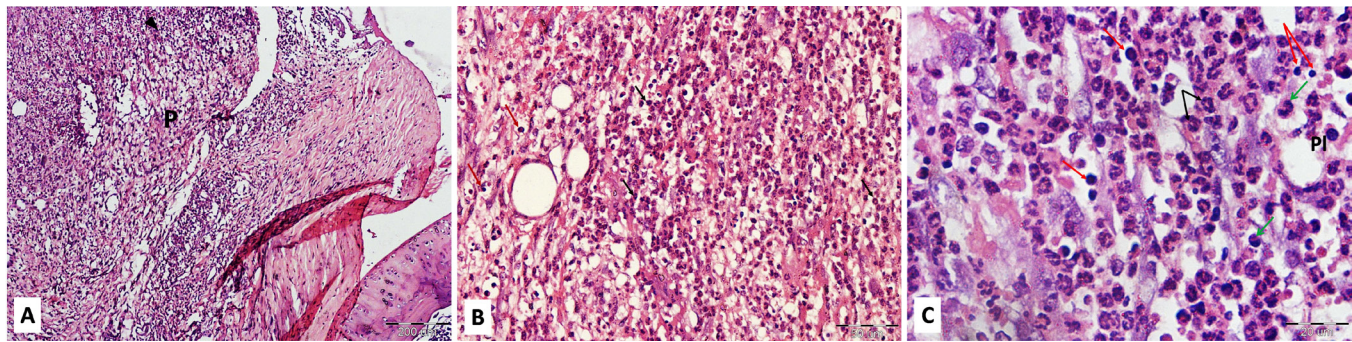


Fig. 12: (A-C): Representative LM pictures of the H & E stained sections of the RA model group II A; Evident mononuclear cellular infiltration (triangle) is seen within the pannus tissue (P). B & C; Higher magnifications demonstrate abundant cells with multisegmented nuclei suggestive of neutrophils (black arrows), and other cells with large rounded nuclei suggestive of lymphocytes (red arrows). C; Some cells with bilobed nuclei (green arrows), characteristic of eosinophils, are exhibited. An oval cell that displays an eccentric nucleus with cart-wheel chromatin pattern (PI) is observed, suggestive of plasma cell. Mic Mag A x 100, B x 400, C x 1000.

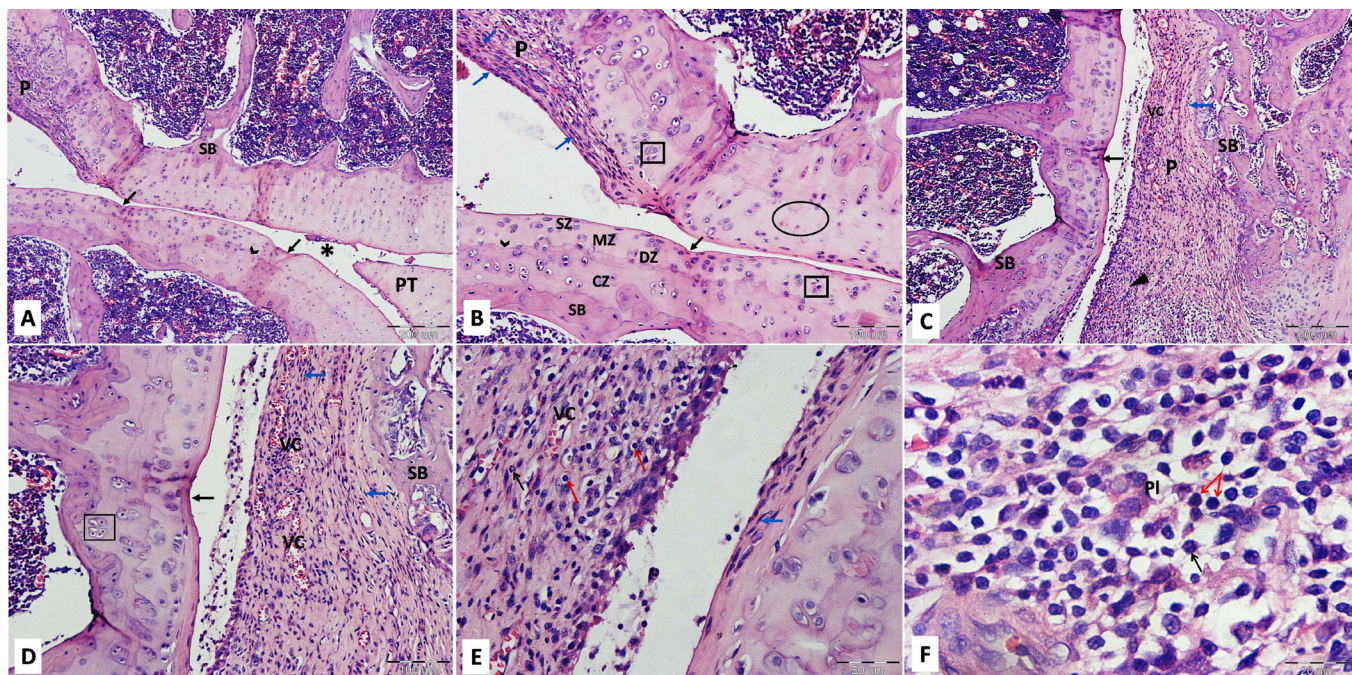


Fig. 13: (A-F): Representative LM pictures of the H & E stained sections of the GR treated group III. A; Partially preserved joint space (asterisk) is observed with apparent patella (PT). A & B; Articular cartilage surface shows some irregularities (black arrows). Limited pannus (P) invasion is observed with abundant fibroblasts (blue arrows). B; Articular cartilage depicts distinct zones (SZ, MZ, DZ, CZ) and intact subchondral bone (SB). Cartilage matrix mostly displays homogenous matrix with frequently observed chondrocytes forming cells nests (rectangle). Focal areas exhibit hypocellularity with indistinct tide mark (oval shape). Mic Mag A x 100, B x 200. C & D; Marked pannus (P) invasion is observed with erosion of the articular cartilage surface on one side and focal irregularities (black arrow) on the other. Pannus (P) depicts vascular congestion (VC), mononuclear cellular infiltration (triangle) and apparently abundant fibroblasts (blue arrows). Chondrocytes cell nests are observed (rectangle). SB; subchondral bone. Mic Mag C x 100, D x 200. E; The higher magnification reveals pannus tissue (P) with some cells that depict rounded nuclei suggestive of lymphocytes (red arrows), spindle shaped cells with flat nuclei (fibroblasts) (blue arrows) and rarely observed neutrophils (black arrow). VC; vascular congestion. F; A higher magnification of the cellular infiltration in pannus, exhibiting some cells with cart-wheel chromatin pattern of the nucleus, suggestive of plasma cells (PI), cells with rounded nuclei, suggestive of lymphocytes (red arrows) and one neutrophil (black arrow). Mic Mag E x 400, F x 1000.

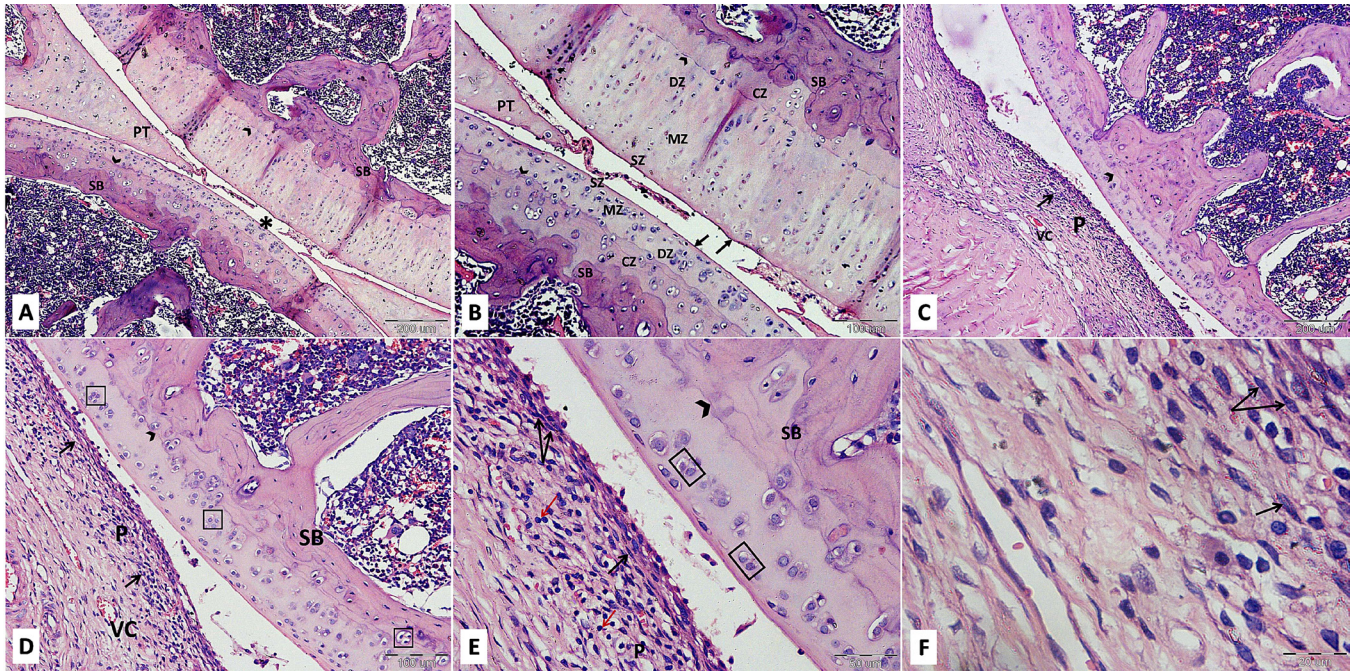


Fig. 14: (A-F): Representative LM pictures of the H & E stained sections of the GAS treated group IV. A; Preserved joint space (asterisk) is observed with apparent tidemark (arrowhead). PT; patella, SB; subchondral bone. B; Higher magnification of picture (A), reveals regular surface of articular cartilage (arrows) with distinct zones (SZ, MZ, DZ, CZ). Evident tidemark (arrowhead) is observed. SB; subchondral bone. Mic Mag A x 100, B x 200. C-E; The joint space appears invaded by pannus tissue (P) that exhibits cellular infiltration (arrows) and vascular congestion (VC). Evident tidemark (arrowhead) is observed. D & E (higher magnifications of picture C); The cartilage matrix depicts abundant chondrocytes with formation of cell nests (rectangle). SB; subchondral bone. E & F (higher magnifications of picture C); revealing abundant fibroblasts (black arrows) within the pannus (P). Few cells with large rounded nuclei (red arrows), suggestive of lymphocytes, are observed in picture E. Mic Mag C x 100, D x 200, E x 400, F x 1000.

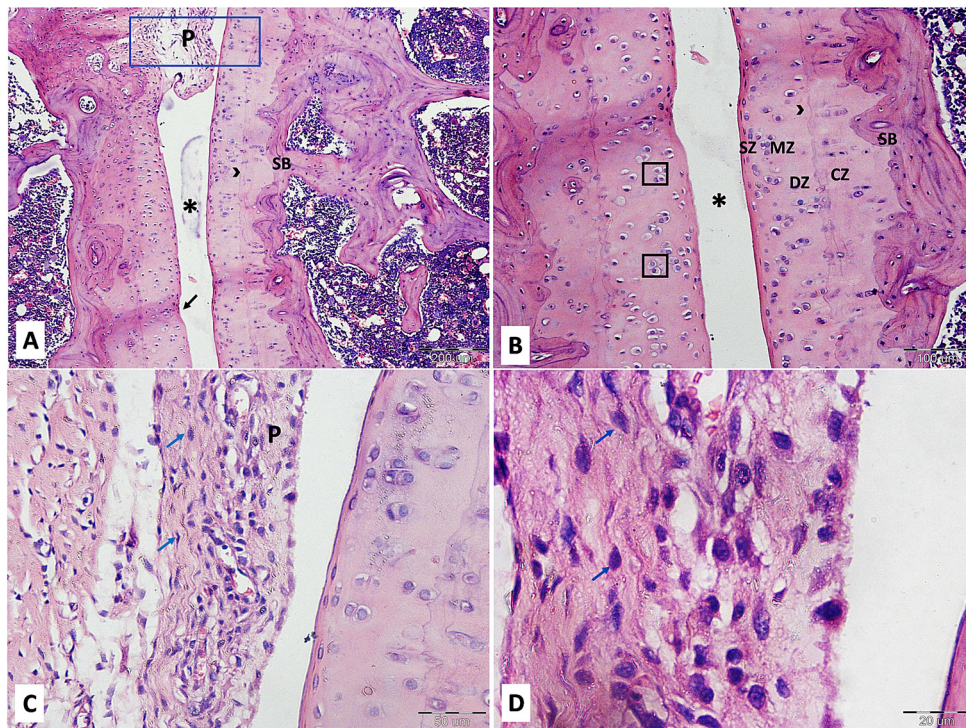


Fig. 15: (A -D): Representative LM pictures of the H & E stained sections of the combined treated group V. A & B; Joint space (asterisk) appears preserved. Limited pannus (P) infiltration is observed. Articular cartilage surface displays mild irregularity (arrow). B is a higher magnifications of picture (A); Different zones of the articular cartilage (SZ, MZ, DZ, CZ & SB) and tide mark (arrowhead) are distinguished. Chondrocytes in cell nests (outlined in rectangle) are observed. C & D (higher magnification of outlined area in the blue rectangle in A); reveals spindle shaped cells (fibroblasts) (blue arrows) within the pannus (P). Mic Mag A x 100, B x 200, C x 400, D x 400, E x 1000.

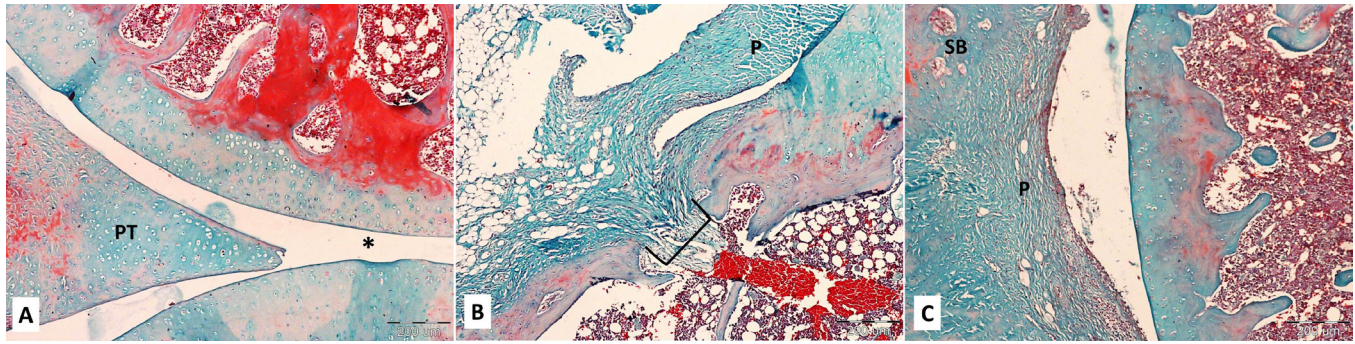


Fig. 16: (A-C): Representative LM pictures of the Masson's trichrome stained sections of the control group (A) and the RA group (B & C). A; The control joint space appears empty (asterisk) with no Masson's trichrome staining, indicating absence of any fibrous tissue. PT; patella. B & C; In the RA group, extensive green stained collagen fibers deposition is observed within pannus tissue (P), replacing the interrupted cartilage (bracket) and overlying the subchondral bone (SB). Mic Mag A-C x 100.

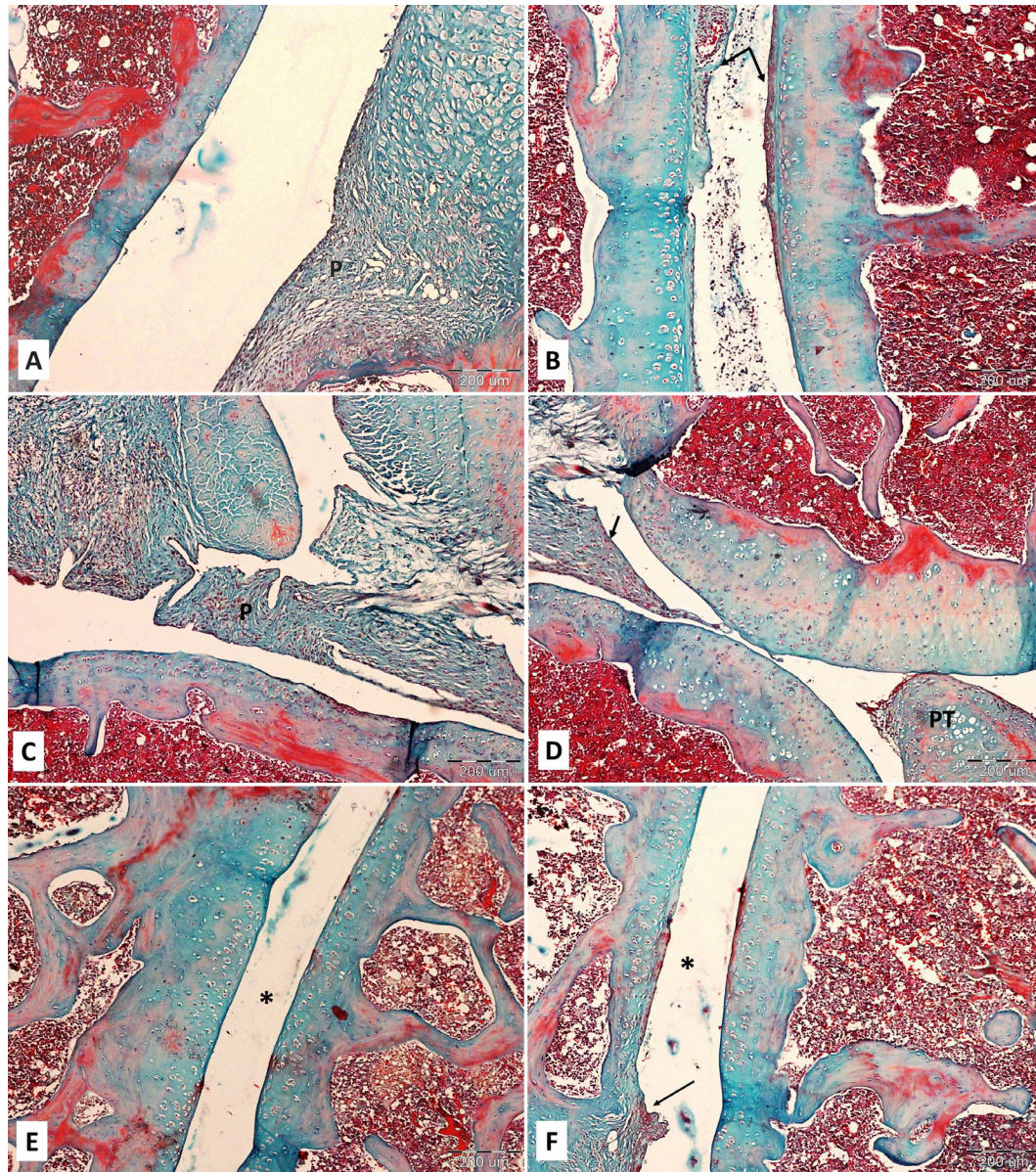


Fig. 17: (A-F): Representative LM pictures of the Masson's trichrome stained sections of the GR group (A & B), the GAS group (C & D), and the combined treatment group (E & F). A & B; In the GR group, evident green stained collagen fibers within the pannus tissue (P) is detected within the joint cavity in figure A, while in the other section in figure B, regression of the collagen fibers deposition is noticed (arrows). C & D; In the GAS group, marked green stained collagen fibers within the pannus tissue (P) is seen occupying the joint cavity in figure (C). However, limitation of the collagen deposition is apparent in figure (D) (arrows). PT; patella. E & F; The combined treatment group shows marked improvement regarding the fibrous tissue formation within the joint cavity (asterisks), as only focal region of pannus is detected (arrow) in figure F. Mic Mag A-F x 100.

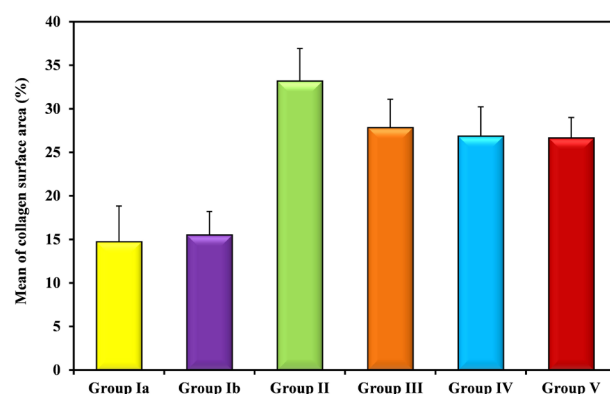


Fig. 18: Bar chart for comparison between the different studied groups according to collagen surface area (%)

Table 1: Comparison between the different studied groups according to serum IL-6 (pg/ml)

| | Group IA (n = 5) | Group IB (n = 5) | Group II (n = 5) | Group III (n = 5) | Group IV (n = 5) | Group V (n = 5) | F (p) |
|-----------------------------|---------------------|---------------------|---------------------|---|---------------------|--------------------|------------|
| IL-6 (pg/ml) | | | | | | | |
| Min. – Max. | 58.0 – 70.0 | 60.0 – 72.0 | 144.0 – 174.0 | 115.0 – 128.0 | 90.0 – 110.0 | 77.0 – 84.0 | F=130.926* |
| Mean ± SD. | 64.60 ± 5.13 | 65.0 ± 4.64 | 161.2 ± 12.11 | 121.2 ± 4.97 | 100.8 ± 9.09 | 79.80 ± 2.77 | (p<0.001*) |
| P ₀ | | 1.000 | <0.001* | <0.001* | <0.001* | 0.029* | |
| P ₁ | | | <0.001* | <0.001* | <0.001* | 0.035* | |
| Significance between groups | | | | p ₂ <0.001*, p ₃ <0.001*, p ₄ <0.001*, p ₅ =0.002*, p ₆ <0.001*, p ₇ =0.001* | | | |

SD: Standard deviation

F: F for One way ANOVA test, Pairwise comparison between each 2 groups was done using Post Hoc Test (Tukey)

p: p value for comparing between the studied groups

p₀: p value for comparing between Group IA and each other group

p₁: p value for comparing between Group IB and each other group

p₂: p value for comparing between Group II and Group III

p₃: p value for comparing between Group II and Group IV

p₄: p value for comparing between Group II and Group V

p₅: p value for comparing between Group III and Group IV

p₆: p value for comparing between Group III and Group V

p₇: p value for comparing between Group IV and Group V

*: Statistically significant at p ≤ 0.05

Table 2: Comparison between the different studied groups according to serum TNF-α (pg/ml)

| | Group IA (n = 5) | Group IB (n = 5) | Group II (n = 5) | Group III (n = 5) | Group IV (n = 5) | Group V (n = 5) | F (p) |
|-----------------------------|---------------------|---------------------|---------------------|----------------------|---|--------------------|------------|
| TNF-α (pg/ml) | | | | | | | |
| Min. – Max. | 44.0 – 60.0 | 47.0 – 63.0 | 102.0 – 130.0 | 92.0 – 107.0 | 70.0 – 84.0 | 53.0 – 64.0 | F=70.581* |
| Mean ± SD. | 52.0 ± 6.32 | 57.60 ± 6.47 | 117.0 ± 10.68 | 99.40 ± 6.27 | 76.60 ± 6.07 | 58.40 ± 4.62 | (p<0.001*) |
| P ₀ | | 0.800 | <0.001* | <0.001* | <0.001* | 0.699 | |
| P ₁ | | | <0.001* | <0.001* | 0.003* | 1.000 | |
| Significance between groups | | | | | p ₂ =0.006*, p ₃ <0.001*, p ₄ <0.001*, p ₅ <0.001*, p ₆ <0.001*, p ₇ =0.005* | | |

SD: Standard deviation

F: F for One way ANOVA test, Pairwise comparison between each 2 groups was done using Post Hoc Test (Tukey)

p: p value for comparing between the studied groups

p₀: p value for comparing between Group IA and each other group

p₁: p value for comparing between Group IB and each other group

p₂: p value for comparing between Group II and Group III

p₃: p value for comparing between Group II and Group IV

p₄: p value for comparing between Group II and Group V

p₅: p value for comparing between Group III and Group IV

p₆: p value for comparing between Group III and Group V

p₇: p value for comparing between Group IV and Group V

*: Statistically significant at p ≤ 0.05

Table 3: Comparison between the different groups according to gross anatomical results

| Gross anatomical results | Group IA | Group IB | Group II | Group III | Group IV | Group V | H | p |
|--------------------------|------------------|------------------|--------------------------|---------------------------|--------------------------|---------------------------------|---------|---------|
| Mean ± SD | 0.0 ± 0.0 | 0.0 ± 0.0 | 3.80 [#] ± 0.63 | 2.30 ^{#@} ± 0.67 | 2.0 ^{#@} ± 0.47 | 0.80 ^{@\$&} ± 0.42 | | |
| Median (Min.- Max.) | 0.0 (0.0-0.0) | 0.0 (0.0-0.0) | 4.0 (3.0-5.0) | 2.0 (1.0-3.0) | 2.0 (1.0-3.0) | 1.0 (0.0-1.0) | 43.852* | <0.001* |

H: H for Kruskal Wallis test, Pairwise comparison between each 2 groups was done using Post Hoc Test (Dunn's for multiple comparisons test)

#: Significant with group IA or IB

@: Significant with group II

\$: Significant with group III

&: Significant with group IV

*: Statistically significant at $p \leq 0.05$

Table 4: Comparison between the different studied groups according to collagen surface area (%)

| | Group IA (n = 5) | Group IB (n = 5) | Group II (n = 5) | Group III (n = 5) | Group IV (n = 5) | Group V (n = 5) | F (p) |
|------------------------------|---------------------|---------------------|---|----------------------|---------------------|--------------------|-------------------------|
| Collagen surface area (%) | | | | | | | |
| Min. – Max. | 10.97 – 21.53 | 13.05 – 20.11 | 28.33 – 38.52 | 24.39 – 32.45 | 23.83 – 31.76 | 23.92 – 29.25 | F=25.019* (p<0.001*) |
| Mean ± SD. | 14.73 ± 4.10 | 15.52 ± 2.70 | 33.20 ± 3.73 | 27.84 ± 3.26 | 26.88 ± 3.34 | 26.65 ± 2.35 | |
| P ₀ | | 0.999 | <0.001* | <0.001* | <0.001* | <0.001* | |
| P ₁ | | | <0.001* | <0.001* | <0.001* | 0.001* | |
| Significance bet groups | | | p ₂ =0.145, p ₃ =0.057, p ₄ =0.045*, p ₅ =0.997, p ₆ =0.992, p ₇ =1.000 | | | | |

SD: Standard deviation

F: F for One way ANOVA test, Pairwise comparison between each 2 groups was done using Post Hoc Test (Tukey)

p: p value for comparing between the studied groups

p₀: p value for comparing between Group IA and each other group

p₁: p value for comparing between Group IB and each other group

p₂: p value for comparing between Group II and Group III

p₃: p value for comparing between Group II and Group IV

p₄: p value for comparing between Group II and Group V

p₅: p value for comparing between Group III and Group IV

p₆: p value for comparing between Group III and Group V

p₇: p value for comparing between Group IV and Group V

*: Statistically significant at $p \leq 0.05$

DISCUSSION

Nowadays, rheumatoid arthritis represents a vital field for the research studies due to its impact on the human health and its associated limitations of physical abilities, the issues that adversely affects the quality of life^[2].

In the present study, CFA was used for induction of adjuvant-induced arthritis (AIA) in a rat model, as it was documented by previous research work to be a convenient model for studying the different parameters involved in the RA pathogenesis, and eventually allowing for experimental implementation of variable therapeutic strategies^[15].

Accomplishment of RA in the current study was confirmed biochemically, anatomically and histologically.

Biochemically, the serum levels of IL-6 and TNF- α were markedly elevated in the RA group, thus indicating an inflammatory reaction. Such results come in agreement with results of a study by El Ghazaly *et al.*^[29] The gross joint examination revealed articular cartilage surface distortion that was confirmed by SEM examination, where evident surface irregularities were observed. Additionally, light microscopic examination results were in context through observation of articular surface irregularities, erosions by

the invading pannus, together with inflammatory cellular infiltration within the synovial tissue. In addition, variable degenerative changes were encountered in the form of degenerating chondrocytes and areas of hypocellularity within the matrix. Such findings come in agreement with Liu *et al.*^[15] who reported similar findings in CFA induced arthritis male Sprague-Dawley rats' model.

RA is an autoimmune inflammatory disorder that involves an interplay of several factors, including alternation of cytokines generation, where TNF- α is reported to play a crucial role. Increased production of TNF- α in the joint and serum induces expansion of the synovial membrane fibroblasts, together with enhanced prostaglandin-E2 production, hence triggering production of other cytokines and accentuation of the inflammatory reaction^[30-32]. Furthermore, enhanced transcription of nuclear factor kappa beta (NF- κ B) by TNF- α represents a significant step that results in additional pro-inflammatory cytokines production^[29].

It is also worth mentioning that the mycobacterium in CFA stimulates neutrophils infiltration into the synovium, where neutrophils secrete more TNF- α and other pro-inflammatory cytokines, such as, IL-6 and IL-4. Moreover,

neutrophils result in a robust of reactive oxygen species (ROS) production, with a subsequent generation of oxidative stress within the joint tissue^[29,33,34].

In addition, a study conducted by Huang *et al.*^[35] reported that synovial fibroblasts produce TNF- α as well. In addition, several previous studies have confirmed the role of synovial fibroblasts in RA pathogenesis^[15,36].

As such, the observed increased fibroblasts in the synovium in the H & E stained sections of the RA group is justified. Subsequently increased collagen deposition occurs within the synovium, thereby leading to pannus tissue formation that extends into the joint space, overlying the articular cartilage surface. This comes in accordance with the histological results of the H & E stained sections, that revealed pannus tissue invading the joint space and even encroaching on the cartilage surface, causing focal areas of discontinuity of cartilage surface. Masson's trichrome stained sections of RA group further confirmed the increased collagen deposition within the synovium of the RA group that was significant as compared to the control group.

The encountered erosions in cartilage matrix can be referred also to the effect of matrix metalloproteinases (MPPs), that are released by the proliferated synovial fibroblasts and the chondrocytes in response to TNF- α ^[37].

As regards the degenerative changes depicted by the chondrocytes, it is suggested that they are induced by the state of oxidative stress, where membrane lipid peroxidation deranges cell membrane transport mechanism with subsequent cytoplasmic vacuolization. Meanwhile, the generated free radicals cause nuclear damage and eventually chondrocytes necrosis^[38]. Hence, the observed areas of hypocellularity within the cartilage matrix, together with the vacuolated chondrocytes with dark small nuclei, are verified.

The inflammatory reaction was further supported by the observed vascular congestion and neutrophilic infiltration. This comes in line with the study of Arafa *et al.*^[36] who demonstrated that number of blood vessels within the pannus correlates positively with mononuclear cellular infiltration. Interestingly, lymphocytes and plasma cells were observed within the inflammatory cellular infiltration, the issue that supports the autoimmune mechanism involved in RA pathogenesis.

Early therapeutic intervention is thus mandatory to hinder the possible complications of RA and provide an opportunity for commencement of the regenerative and healing processes. Thereby, implementation of therapeutic regimens that target the variable factors involved in the pathogenesis was applied in the current study.

Long time ago, GR was regarded within the scope of the traditional medicine and had been recommended for patients with arthritis and muscle pain. It is not surprising, as it has protective effects against joints and musculoskeletal disorders, via its strong anti-inflammatory, antioxidant, and anti-serotonin influences^[39].

The anti-inflammatory effects of ginger are related to its ability to inhibit the phosphorylated-JAK-3 protein, thereby abating the secretion of several pro-inflammatory cytokines and inflammation-related mediators^[40]. In addition, it could block cyclooxygenase-2, NF- κ B and 5-lipoxygenase signaling inflammatory pathways^[41]. These effects result in reduction of several serum and synovial fluid inflammatory markers, such as NO, TNF α , IL1 β , IL6, prostaglandins, monocyte chemoattractant protein-1 (MCP-1), C-reactive protein and substance P^[39,42].

At the same time, GR induces production of numerous anti-inflammatory cytokines such as IL-4 and IL-10, and enhances the activity of antioxidant factors like superoxide dismutase, CAT and GSH, leading to depression of the oxidative stress and free radicals^[41,43].

The results of the present study correlates positively with the aforementioned anti-inflammatory influence of GR, where there was a significant decline in the serum levels of TNF- α and IL-6 as compared to the RA group. Gross examination and SEM results revealed relative improvement, where articular cartilage surface irregularities were less pronounced as compared to the RA group. Histologically, partial amelioration of inflammatory signs was observed in the GR treated group. Herein, decreased inflammatory cellular infiltration and vascular congestion were encountered, together with regression of the pannus tissue in some sections. Moreover, the morphometric analysis of Masson's trichrome stained sections revealed decreased collagen deposition in comparison to RA group but not significantly. Nevertheless, the antioxidant effect of GR was justified histologically through the observed increased chondrocytes and cell nests, indicating the restored proliferative ability of the chondrocytes.

Additionally, it is postulated that GR can modulate the immune function in RA through decreasing T-cell and B-cell proliferation, thus leading to immunological enhancement and attenuation of RA effects^[40].

Moreover, GR decreases the expression of T-bet gene (T-box expressed in T cells) significantly. T-bet gene is present in T-helper1 (Th-1) cells, and its expression induces their proliferation. Ginger also inhibits T-helper 2 (Th-2) differentiation. Moreover, Ginger has shown to down regulate the expression of B71, B72 and MHC class II molecules, resulting in inhibition of the antigen-presenting activity of macrophages and T cells^[1,41].

Lu *et al.*^[44] have documented that, GR could not only suppress the activation of T cells, but also the B cells. It significantly decreases differentiation of B cells, and production of IgG-1 and IgG-2b at a concentration dependent manner. Also, GR augments expression of FoxP3 (forkhead box P3) gene, thus indicating the immune-modulatory effects of this plant. FoxP3 is a transcription factor in T-reg cells, and its increase causes a subsequent increase in T-reg cells function and modulation of the immune system. These results suggest that GR has strong immunosuppressive effects on humoral and cellular immune responses^[41].

Furthermore, GR increases PPAR- γ (peroxisome proliferator-activated receptor- γ) gene expression. PPAR- γ agonists have been shown to suppress translation of genes involved in joint pathology such as gelatinase-B, MMP-9,13^[45]. This comes in agreement with our histological results that demonstrated a restored articular cartilage matrix integrity in some H & E stained sections.

As regards glucosamine, which is a naturally occurring amino-monosaccharide, it is the preferred substrate for the biosynthesis of proteoglycans. It has been documented to play major roles in cartilage formation, repair, maintenance of cartilage integrity, and in joint tissue remodeling^[6,46].

In the present study, IL-6, and TNF- α levels were significantly inhibited by GAS. Such a finding was in correlation with Aghazadeh-Habashi *et al.*^[47] who had analyzed the effects of glucosamine in rats, and found that only 6-days glucosamine supplementation has reduced the levels of proinflammatory cytokines IL-1 β , IL-6, C-reactive protein and TNF- α , and upregulated the anti-inflammatory cytokine IL-2. Mechanistically, glucosamine inhibits the activation of the nuclear factor $\kappa\beta$ (NF- $\kappa\beta$) and p38 mitogen-activated protein kinase (MAPK) inflammatory pathways^[48].

Gross and histological results further confirmed the biochemical results, where evident amelioration of the degenerative and the inflammatory changes were encountered in the GAS group. Additionally, morphometric analysis of Masson's trichrome stained sections, demonstrated decreased collagen within the synovium, thus being in context with the observed decreased cellular infiltration in the H & E stained sections.

In addition, GAS has a significant free radical-scavenging activity and an ability to inhibit membrane lipid peroxidation. In the articular cartilage, it effectively reduces oxidative stress and the intracellular ROS level in the chondrocytes. Such an effect is mediated through its direct binding to malondialdehyde (MDA), an important byproduct of membrane lipid peroxidation. Moreover, it remarkably prevents lipopolysaccharide (LPS)-induced ROS generation and caspase-1 activation in the chondrocytes^[49]. Furthermore, it could inhibit hydrogen peroxide (H₂O₂)-mediated membrane lipid peroxidation and DNA oxidation in the chondrocytes. On the other hand, glucosamine can upregulate GSH and several antioxidant enzymes, including SOD, CAT, and glutathione peroxidases^[48]. Wu. S *et al.*^[50], reported also that, oral intake of GAS has reduced plasma MDA and inducible nitric oxide synthase (iNOS) enzymes, NO, and PGE-2 levels in chemically induced rheumatoid arthritis in albino rats. Such an antioxidant effect was revealed in the current study, where chondrocytes mostly restored normal histological features.

On the genetic level, MMP-3 in patients with RA were reduced by treatment with glucosamine. MMP-3 (produced by synovium-lining cells and chondrocytes) activates pro-collagenases, leading to destruction of cartilage

proteoglycans^[51]. In addition, glucosamine reduces gene expression of MMP-13 and Col3a1 (collagenase-3a1) genes, which encode for proteases of the extracellular matrix proteins and type III collagen. Accordingly, glucosamine can prevent the degradation of cartilage matrix proteins and replacement of type II collagen with type III collagen during the early stages of fibrosis of the synovial tissues^[37].

Collectively, we can consider that, glucosamine has strong tissue regeneration capacity and chondro-protective effect. It increases deposition of collagen type II, aggrecan, and GAGs. Moreover, it enhances the chondrogenic differentiation and synovial fluid stem cells proliferation. However, it decreases deposition of collagen type I, fibrocartilage formation and chondrocytes calcium deposition^[48]. In this context, the relative observed improvement grossly and histologically is explained, where homogenous intact matrix with well-defined articular cartilage zones, together with abundant chondrocytes and cell nests, were encountered in the H & E stained sections.

In our results, the combined treatment with GR and GAS, revealed the most pronounced anti-inflammatory effect, where a significant decrease in serum levels of IL-6 and TNF- α was achieved, restoring nearly the control values. This finding was confirmed with the gross macroscopic, scanning electron microscope and histological examination of the knee joint that revealed mostly normal features, except for limited changes. In addition, morphometric analysis of collagen area percentage, revealed a significant decreased value as compared to the RA group, thereby presenting a potent therapeutic effect of the combined treatment strategy. This comes in agreement with Abd El-Ghany *et al.*^[43], who demonstrated the maximum improvement of a model of monosodium iodoacetate-induced osteoarthritis, with implementation of a combination of GAS and GR.

CONCLUSION

It can be concluded that the administration of both GAS and GR together has a synergetic effect, and together they could ameliorate RA more potently. Accordingly, it is recommended to apply the combined therapeutic regimen in treatment of RA to enhance the healing process and avoid irreversible tissue damage. In addition, further studies are essential to elucidate the possible protective effect of GR or/and GAS in high risk patients to ameliorate or even prevent the disease pathogenesis.

ETHICAL STATEMENT

The animal studies were performed after receiving approval of the institutional review board of ethics, Faculty of Medicine, Alexandria University.

ACKNOWLEDGMENTS

The authors appreciate the supportive role of the Faculty of Medicine, Alexandria University.

CONFLICT OF INTERESTS

There are no conflicts of interest.

REFERENCES

1. Lindler BN, Long KE, Taylor NA and Lei W: Use of Herbal Medications for Treatment of Osteoarthritis and Rheumatoid Arthritis. *Medicines* (Basel, Switzerland) (2020) 7(11):67. doi: 10.3390/medicines7110067
2. Derksen V, Huizinga TWJ and van der Woude D: The role of autoantibodies in the pathophysiology of rheumatoid arthritis. *Semin. Immunopathol.* (2017) 39(4):437-446. doi.org/10.1007/s00281-017-0627-z
3. Ruffing V and Bingham CO: Rheumatoid Arthritis Signs and Symptoms. 2016. Available from: <https://www.hopkinsarthritis.org/arthritis-info/rheumatoid-arthritis/ra-symptoms/> [Accessed in: May, 2022].
4. Curtis JR and Singh JA: Use of biologics in rheumatoid arthritis: current and emerging paradigms of care. *Clin. Ther.* (2011) 33(6):679-707. doi: 10.1016/j.clinthera.2011.05.044
5. Sasane P, Saroj UR and Joshi RK: Clinical evaluation of efficacy of Alambushadi Ghana Vati and Vaitarana Basti in the management of Amavata with special reference to rheumatoid arthritis. *Ayu* (2016) 37(2):105-112. doi: 10.4103/ayu.AYU_91_15
6. Dai W, Qi C and Wang S: Synergistic effect of glucosamine and vitamin E against experimental rheumatoid arthritis in neonatal rats. *Biomed Pharmacother.* (2018) 105:835-840. doi.org/10.1016/j.biopha.2018.05.136
7. Kolasinski SL, Neogi T, Hochberg MC, *et al*: 2019 American College of Rheumatology/Arthritis Foundation Guideline for the Management of Osteoarthritis of the Hand, Hip, and Knee. *Arthritis Rheumatol.* (2020) 72(2):220-233. doi.org/10.1002/art.41142
8. Singh JA, Saag KG, Bridges SL, Jr., *et al*: 2015 American College of Rheumatology Guideline for the Treatment of Rheumatoid Arthritis. *Arthritis Care Res. (Hoboken)* (2016) 68(1):1-25. doi.org/10.1002/art.39480
9. Wasserman AM: Diagnosis and management of rheumatoid arthritis. *Am. Fam. Physician* (2011) 84(11):1245-1252.
10. Reginster JY, Neuprez A, Lecart MP, Sarlet N and Bruyere O: Role of glucosamine in the treatment for osteoarthritis. *Rheumatol. Int.* (2012) 32(10):2959-2967. doi: 10.1007/s00296-012-2416-2
11. Bruyère O, Reginster JY, Honvo G and Detilleux J: Cost-effectiveness evaluation of glucosamine for osteoarthritis based on simulation of individual patient data obtained from aggregated data in published studies. *Aging Clin Exp Res* (2019) 31(6):881-887. doi: 10.1007/s40520-019-01138-1
12. Ogata T, Ideno Y, Akai M, *et al*: Effects of glucosamine in patients with osteoarthritis of the knee: a systematic review and meta-analysis. *Clin Rheumatol* (2018) 37(9):2479-2487. doi: 10.1007/s10067-018-4106-2
13. Ghasemzadeh A, Jaafar HZ and Rahmat A: Antioxidant activities, total phenolics and flavonoids content in two varieties of Malaysia young ginger (*Zingiber officinale* Roscoe). *Molecules* (2010) 15(6):4324-4333. doi.org/10.3390/molecules15064324
14. Mihaylova D, Ivanova M, Bahchevanska S and Krastanov A: Chemical composition and antioxidant activity of ultrasound-assisted extract of the endemic plant *Haberlea rhodopensis* Friv. *J Food Sci Technol* (2015) 52(4):2469-2473. doi: 10.1007/s13197-013-1240-3
15. Liu YL, Lin HM, Zou R, Wu JC, Han R, Raymond LN, Reid PF and Qin ZH: Suppression of complete Freund's adjuvant-induced adjuvant arthritis by cobratoxin. *Acta Pharmacol. Sin.* (2009) 30(2):219-227. doi: 10.1038/aps.2008.20
16. Aborehab NM, El Bishbishy MH, Refaiy A and Waly NE: A putative Chondroprotective role for IL-1 β and MPO in herbal treatment of experimental osteoarthritis. *BMC Complement. Altern. Med.* (2017) 17(1):495. doi: 10.1186/s12906-017-2002-y
17. Ali SM, Okda AAK, Dessouky IS, Hewedy WA, Zahran NM and Alamrani BA-w: l-Carnitine ameliorates knee lesions in mono-iodoacetate induced osteoarthritis in rats. *Alex. J. Med.* (2017) 53(1):61-66. doi.org/10.1016/j.ajme.2016.03.002
18. Bernotiene E, Bagdonas E, Kirdaite G, *et al*: Emerging Technologies and Platforms for the Immunodetection of Multiple Biochemical Markers in Osteoarthritis Research and Therapy. *Front Med (Lausanne)* (2020) 7:572977. doi: 10.3389/fmed.2020.572977
19. Juhász K, Buzás K and Duda E: Importance of reverse signaling of the TNF superfamily in immune regulation. *Expert Rev Clin Immunol* (2013) 9(4):335-348. doi.org/10.1586/eci.13.14
20. Ängeby Möller K, Klein S, Seeliger F, Finn A, Stenfors C and Svensson CI: Monosodium iodoacetate-induced monoarthritis develops differently in knee versus ankle joint in rats. *Neurobiol Pain* (2019) 6:100036. doi: 10.1016/j.ynpai.2019.100036
21. Hermeto LC, DeRossi R, Oliveira RJ, *et al*: Effects of intra-articular injection of mesenchymal stem cells associated with platelet-rich plasma in a rabbit model of osteoarthritis. *Genet. Mol. Res.* (2016) 15(3):1-14. doi.org/10.4238/gmr.15038569
22. Kwon DR, Park GY and Lee SU: The effects of intra-articular platelet-rich plasma injection according to the severity of collagenase-induced knee osteoarthritis in a rabbit model. *Ann. Rehabil. Med.* (2012) 36(4):458-465. doi.org/10.5535/arm.2012.36.4.458

23. Kim SB, Kwon DR, Kwak H, Shin YB, Han HJ, Lee JH and Choi SH: Additive effects of intra-articular injection of growth hormone and hyaluronic acid in rabbit model of collagenase-induced osteoarthritis. *J Korean Med Sci* (2010) 25(5):776-780. doi: 10.3346/jkms.2010.25.5.776
24. Tahmasebi P, Javadpour F and Sahimi M: Three-Dimensional Stochastic Characterization of Shale SEM Images. *Transp. Porous Media* (2015) 110(3):521-531. doi.org/10.1007/s11242-015-0570-1
25. Wang Z, Zhai C, Fei H, Hu J, Cui W, Wang Z, Li Z and Fan W: Intraarticular injection autologous platelet-rich plasma and bone marrow concentrate in a goat osteoarthritis model. *J. Orthop. Res.* (2018) 36(8):2140-6 doi: 10.1002/jor.23877.
26. Azizi S, Farsinejad A, Kheirandish R and Fatemi H: Intra-articular effects of combined xenogenous serum rich in growth factors (SRGF) and vitamin C on histopathology grading and staging of osteoarthritis in rat model. *Transfus Clin Biol* (2019) 26(1):3-9. doi.org/10.1016/j.traccli.2018.08.156
27. Zahran NM, Ahmed WA, Mady BA and Kelada MN: Effects of intra-articular corticosteroid versus platelet-rich plasma on induced knee osteoarthritis in adult albino rats. Histological and anatomical study. *Egypt. J. Histol.* (2021) 45(2):468-587. doi: 10.21608/EJH.22021.70354.21455.
28. Serdar CC, Cihan M, Yücel D and Serdar MA: Sample size, power and effect size revisited: simplified and practical approaches in pre-clinical, clinical and laboratory studies. *Biochem. Med.(Zagreb)* (2021) 31(1):010502. doi: 10.11613/BM.2021.010502
29. El-Ghazaly MA, Fadel NA, Abdel-Naby DH, Abd El-Rehim HA, Zaki HF and Kenawy SA: Potential anti-inflammatory action of resveratrol and piperine in adjuvant-induced arthritis: Effect on pro-inflammatory cytokines and oxidative stress biomarkers. *Egypt. Rheumatol.* (2020) 42(1):71-77. doi.org/10.1016/j.ejr.2019.08.003
30. Farrugia M and Baron B: The role of TNF- α in rheumatoid arthritis: a focus on regulatory T cells. *J Clin Transl Res* (2016) 2(3):84-90.
31. Lopez-Pedreira C, Barbarroja N, Patiño-Trives AM, Luque-Tévar M, Collantes-Estevez E, Escudero-Contreras A and Pérez-Sánchez C: Effects of Biological Therapies on Molecular Features of Rheumatoid Arthritis. *Int J Mol Sci* (2020) 21(23):9067. doi: 10.3390/ijms21239067
32. Makuch S, Więcek K and Woźniak M: The Immunomodulatory and Anti-Inflammatory Effect of Curcumin on Immune Cell Populations, Cytokines, and *In Vivo* Models of Rheumatoid Arthritis. *Pharmaceuticals (Basel)* (2021) 14(4):309. doi.org/10.3390/ph14040309.
33. Gideon HP, Phuah J, Junecko BA and Mattila JT: Neutrophils express pro- and anti-inflammatory cytokines in granulomas from *Mycobacterium tuberculosis*-infected cynomolgus macaques. *Mucosal Immunol.* (2019) 12(6):1370-1381. doi: 10.1038/s41385-019-0195-8
34. Tamassia N, Bianchetto-Aguilera F, Arruda-Silva F, Gardiman E, Gasperini S, Calzetti F and Cassatella MA: Cytokine production by human neutrophils: Revisiting the "dark side of the moon". *Eur. J. Clin. Invest.* (2018) 48 Suppl 2:e12952. doi.org/10.1111/eci.12952
35. Huang CC, Chiou CH, Liu SC, Hu SL, Su CM, Tsai CH and Tang CH: Melatonin attenuates TNF- α and IL-1 β expression in synovial fibroblasts and diminishes cartilage degradation: Implications for the treatment of rheumatoid arthritis. *J. Pineal Res.* (2019) 66(3):e12560. doi.org/10.1111/jpi.12560
36. Arafa NM, Hamuda HM, Melek ST and Darwish SK: The effectiveness of Echinacea extract or composite glucosamine, chondroitin and methyl sulfonyl methane supplements on acute and chronic rheumatoid arthritis rat model. *Toxicol. Ind. Health* (2013) 29(2):187-201. doi.org/10.1177/0748233711428643
37. Kashiuchi S, Miyazawa R, Nagata H, Shirai M, Shimizu M, Sone H and Kamiyama S: Effects of administration of glucosamine and chicken cartilage hydrolysate on rheumatoid arthritis in SKG mice. *Food & Function* (2019) 10(8):5008-5017. doi.org/10.1039/C9FO00981G
38. Kumar V, Abbas A and Aster J: *Robbins Basic Pathology*, Elsevier. London. (2017).
39. Aryaeian N and Tavakkoli H: Ginger and its Effects on Inflammatory Diseases. *Adv. Food Technol. Nutr. Sci. Open J.* (2015) 1(4):97-101. doi.org/10.17140/AFTNSOJ-1-117
40. Zhang YM, Shen J, Zhao JM, Guan J, Wei XR, Miao DY, Li W, Xie YC and Zhao YQ: Cedrol from Ginger Ameliorates Rheumatoid Arthritis via Reducing Inflammation and Selectively Inhibiting JAK3 Phosphorylation. *J. Agric. Food Chem.* (2021) 69(18):5332-5343. doi.org/10.1021/acs.jafc.1c00284
41. Aryaeian N, Shahram F, Mahmoudi M, Tavakoli H, Yousefi B, Arablou T and Jafari Karegar S: The effect of ginger supplementation on some immunity and inflammation intermediate genes expression in patients with active Rheumatoid Arthritis. *Gene* (2019) 698:179-185. doi.org/10.1016/j.gene.2019.01.048
42. Desai A, Shendge PN and Anand SS: Evidence-based nutraceuticals for osteoarthritis: A review. *Int. J. Orthop. Sci.* (2021) 7(2):846-853. doi.org/10.22271/ortho.2021.v7.i2k.2713

43. Abd El-Ghany MA, Ghozy SF and Sultan YM: Therapeutic effects of glucosamine sulfate and ginger extract on monosodium iodoacetate induced osteoarthritis in rats. *Res. J. Specific Educa.* (2018) 2018(50):73-93. doi.org/10.21608/mbse.2018.136866
44. Lu J, Guan S, Shen X, Qian W, Huang G, Deng X and Xie G: Immunosuppressive activity of 8-gingerol on immune responses in mice. *Molecules* (2011) 16(3):2636-2645. doi: 10.3390/molecules16032636
45. Aryaeian N, Mahmoudi M, Shahram F, Poursani S, Jamshidi F and Tavakoli H: The effect of ginger supplementation on IL2, TNF α , and IL1 β cytokines gene expression levels in patients with active rheumatoid arthritis: A randomized controlled trial. *Med. J. Islam. Repub. Iran* (2019) 33:154. doi: 10.34171/mjiri.33.154
46. Li Y, Chen L, Liu Y, Zhang Y, Liang Y and Mei Y: Anti-inflammatory effects in a mouse osteoarthritis model of a mixture of glucosamine and chitooligosaccharides produced by bi-enzyme single-step hydrolysis. *Sci. Rep.* (2018) 8(1):5624. doi.org/10.1038/s41598-018-24050-6
47. Aghazadeh-Habashi A, Kohan MH, Asghar W and Jamali F: Glucosamine dose/concentration-effect correlation in the rat with adjuvant arthritis. *J. Pharm. Sci.* (2014) 103(2):760-767. doi.org/10.1002/jps.23819
48. Al-Saadi HM, Pang K-L, Ima-Nirwana S and Chin K-Y: Multifaceted Protective Role of Glucosamine against Osteoarthritis: Review of Its Molecular Mechanisms. *Sci. Pharm.* (2019) 87(4):34. doi.org/10.3390/scipharm87040034
49. Chiu HW, Li LH, Hsieh CY, Rao YK, Chen FH, Chen A, Ka SM and Hua KF: Glucosamine inhibits IL-1 β expression by preserving mitochondrial integrity and disrupting assembly of the NLRP3 inflammasome. *Sci. Rep.* (2019) 9(1):5603. doi.org/10.1038/s41598-019-42130-z
50. Wu S, Dai X, Shilong F, Zhu M, Shen X, Zhang K and Li S: Antimicrobial and antioxidant capacity of glucosamine-zinc(II) complex via non-enzymatic browning reaction. *Food Sci. Biotechnol.* (2018) 27(1):1-7. doi.org/10.1007/s10068-017-0192-1
51. Zhao JM, Chen X, Cheng K, Shi Q and Peng K: Anserine and glucosamine supplementation attenuates the levels of inflammatory markers in rats with rheumatoid arthritis. *AMB Express* (2020) 10(1):57. doi.org/10.1186/s13568-020-00987-8.

الملخص العربي

التأثير العلاجي المحتمل للزنجبيل و/ أو كبريتات الجلوكوزامين في علاج الإلتهاب المفصلي الروماتويدي المستحث عن طريق العامل المساعد في الجرذان البالغة: دراسة تشريحية و نسيجية وكيميائية حيوية

رحاب أحمد عبد المنعم^١، مروة محمود ماضي^٢، منى حسن فتح الباب^٢، هبة فتحي إبراهيم^١

^١قسم علم الأنسجة وبيولوجيا الخلية، ^٢قسم التشريح، ^٣قسم الكيمياء الحيوية، كلية الطب، جامعة الإسكندرية

مقدمة البحث: يعتبر إلتهاب المفاصل الروماتويدي مشكلة صحية شائعة لها تأثير كبير على جودة الحياة . ومن ثم ، فقد تم إختبار أنظمة علاجية متنوعة لتخفيف الأعراض وإعاقة تقدم المرض .

الهدف من البحث: تقييم التأثير العلاجي للزنجبيل أو كبريتات الجلوكوزامين بشكل منفصل مقابل إعطائهم المشترك في نموذج التهاب المفاصل الروماتويدي المستحث في الجرذان .

مواد وطرق البحث: تم تقسيم ستين من الجرذان البالغة من الإناث إلى خمس مجموعات: المجموعة الأولى المجموعة (الضابطة) تتكون من ٢٠ جرد , بينما الجرذان الاربعين الاخرى فقد تم إحداث إلتهاب المفاصل الروماتويدي في مفصل الركبة عن طريق حقن ١٠٠ ميكروليتر من Complete Freund's Adjuvant داخل كل مفصل لمرة واحدة ، ثم وزعت الجرذان بعد سبعة أيام إلي ٤ مجموعات كالتالي : المجموعة الثانية مجموعة الإلتهاب الروماتويدي ، المجموعة الثالثة مجموعة الزنجبيل (حيث تلقي كل جرد ٤٠٠ مجم من الزنجبيل / كجم / يوم) ، المجموعة الرابعة المجموعة كبريتات الجلوكوزامين (تلقي كل جرد ٢٥٠ مجم من كبريتات الجلوكوزامين / كجم / يوم) ، والمجموعة الخامسة مجموعة المعالجة المشتركة, ثم تم إجراء القتل الرحيم لجرذان كل مجموعات العلاج بعد ٢٨ يومًا.

تم تقييم مستويات TNF- α و IL-6 في الدم ، وتم فصل مفاصل الركبة اليمنى لإجراء فحوصات تشريحية وفحص بالمجهر الإلكتروني الماسح. في حين ان مفاصل الركبة اليسرى تم تحضيرها للفحص النسيجي بواسطة صبغات H & E و Masson's trichrome.

نتائج البحث: في المجموعة الخامسة ، استعادت مستويات TNF- α و IL-6 القيم الطبيعية تقريبًا . وكشفت الفحوصات التشريحية و الفحص بالمجهر الإلكتروني الماسح عن إنتظام الأسطح المفصالية الغضروفية. من الناحية النسيجية ، لوحظ أن الأسطح المفصالية الغضروفية ملساء تقريبًا مع الإحتفاظ بتجويف المفصل وتمييز لطبقات الغضروف ، مقارنةً بالمجموعات المعالجة بالزنجبيل و كبريتات الجلوكوزامين ، والتي أظهرت بعض الشرائح فيها عدم إنتظام لسطح الغضروف وتكاثر للغشاء الزليلي في تجويف المفصل. أظهرت الشرائح المصبوغة بـ Masson's Trichrome إنخفاضًا كبيرًا في النسبة المئوية لمساحة الكولاجين في المجموعة الخامسة مقارنة بمجموعة الإلتهاب المفصلي الروماتويدي.

الاستنتاج: عزز العلاج المشترك التأثير العلاجي للزنجبيل وكبريتات الجلوكوزامين ، وبالتالي تسبب في التحسن الأكبر في جميع القياسات التي تم تقييمها.